bioRxiv preprint doi: https://doi.org/10.1101/248187; this version posted January 28, 2019. The copyright holder for this preprint (which was not certified by peer review) is the author/funder. All rights reserved. No reuse allowed without permission.

PDE5 inhibition improves symptom-free survival and restores transverse tubule loss and catecholamine responsiveness in heart failure

Michael Lawless[1], Jessica L. Caldwell[1], Charlotte E.R. Smith[2], Emma J. Radcliffe[2], George W.P. Madders, David C. Hutchings, Lori S. Woods, Stephanie J. Church[3], Richard D. Unwin[3], Graeme J. Kirkwood, Lorenz K. Becker, Charles M. Pearman, Rebecca F. Taylor, David A. Eisner, Katharine M. Dibb & Andrew. W Trafford*.

[1], contributed equally; [2], contributed equally.

* Correspondence

Unit of Cardiac Physiology and [3.] Centre for Advanced Discovery and Experimental Therapeutics, Division of Cardiovascular Sciences, School of Medical Sciences, Faculty of Biology, Medicine and Health, The University of Manchester, Manchester Academic Health Science Centre, Manchester Academic Health Science Centre, 3.24 Core Technology Facility, 46 Grafton Street, Manchester, M13 9NT,
United Kingdom.

+44 161 275 7969

Andrew.W.Trafford@manchester.ac.uk

bioRxiv preprint doi: https://doi.org/10.1101/248187; this version posted January 28, 2019. The copyright holder for this preprint (which was not certified by peer review) is the author/funder. All rights reserved. No reuse allowed without permission.

Abstract

Heart failure is characterized by poor survival, a loss of catecholamine reserve and cellular structural remodeling in the form of disorganization and loss of the transverse tubule network. Indeed, survival rates for heart failure are worse than many common cancers and have not improved over time. Tadalafil is a clinically relevant drug that blocks phosphodiesterase 5 with high specificity and is used to treat erectile dysfunction. Using a sheep model of advanced heart failure, we show that tadalafil treatment results in a marked improvement in symptom-free survival, reverses transverse tubule loss and restore cardiac myocyte systolic calcium transient amplitude and the hearts chronotropic and contractile response to catecholamines. These effects are independent of changes in myocardial cGMP content and are associated with upregulation of both monomeric and dimerized forms of protein kinase G and of the cGMP hydrolyzing phosphodiesterase 2 and 3. We propose that the molecular switch for the loss of transverse tubules in heart failure and their restoration following tadalafil treatment involves the BAR domain protein Amphiphysin II (BIN1) and the restoration of catecholamine sensitivity is through reductions in G-protein receptor kinase 2, protein phosphatase 1 and protein phosphatase 2A abundance following phosphodiesterase 5 inhibition.

(197 words)

bioRxiv preprint doi: https://doi.org/10.1101/248187; this version posted January 28, 2019. The copyright holder for this preprint (which was not certified by peer review) is the author/funder. All rights reserved. No reuse allowed without permission.

Impaired responsiveness to catecholamines is a hallmark of the failing heart and is detectable both *in vivo* and in isolated ventricular myocytes [1,2]. The mechanisms responsible for the attenuated catecholamine effects in heart failure (HF) are varied and include reduced adenylate cyclase activity and enhanced G protein receptor kinase (GRK2) and intracellular protein phosphatase activity (PP1 and PP2A) which together lead to a decrease in cAMP dependent signaling and impaired PKA-dependent target phosphorylation [1,3,4]. Given the functional distribution of β-adrenergic receptors (β-ARs) and G-proteins across the surface sarcolemma and transverse tubule (TT) membrane [5-7] a further factor proposed to contribute to impairment of the β-adrenergic signalling cascade in HF is the reduction of transverse tubule (TT) density seen in many pre-clinical models and human HF [8-11].

In addition to the classical cAMP-dependent process, the myocardial response to catecholamine stimulation is also regulated by the cGMP-PKG signaling axis consisting of the β_3-AR / soluble guanylate cyclase (sGC) and natriuretic peptide / particulate guanylate cyclase (pGC) pathways (reviewed by Tsai and Kass [12]). The outcome of cGMP dependent activation depends on the source of activating cGMP; that activated by sGC inhibiting the β-AR response whereas pGC derived cGMP has no effect [13,14]. Beyond the role of PKG, GRK2 and protein phosphatases in determining the outcome of β-AR stimulation, the intracellular pools of cAMP and cGMP are also differentially regulated by PDEs suggesting highly compartmentalized regulation of the cyclic nucleotides and thus catecholamine responsiveness of the healthy ventricular myocardium e.g. [15-18].

Given the negative impact of acute PDE5 inhibition on the inotropic and lusitropic response to catecholamines and the established loss of catecholamine reserve in HF it is somewhat surprising that an emerging body of evidence suggests PDE5 inhibition is clinically cardioprotective in type II diabetes [19], left ventricular hypertrophy [20] and in patients with HF with reduced ejection fraction (systolic HF) [21]. Similarly, in experimental models, PDE5 inhibition shows cardioprotective effects in pulmonary hypertension [22], myocardial infarction [23-26] and following aortic banding [27]. However, in each of these cases PDE inhibitor treatment was commenced either before or given concurrently with the disease intervention. Such an experimental approach complicates interpretation of whether the intervention is therapeutically useful in a setting of established disease or acting by preventing disease development. In most [28,29], but not

bioRxiv preprint doi: https://doi.org/10.1101/248187; this version posted January 28, 2019. The copyright holder for this preprint (which was not certified by peer review) is the author/funder. All rights reserved. No reuse allowed without permission.

all [30] experimental studies where PDE5 inhibition has been commenced once some degree of left ventricular remodeling has occurred the findings remain supportive of a cardioprotective effect. However, in the 'positive' studies data on survival outcomes is absent and the extent of disease progression to symptomatic heart failure is unclear. For example, the systolic Ca^{2+} transient in aortic banded animals is at least as large as that observed in sham animals and the Ca^{2+} transient response to β-AR stimulation is greater in the aortic banded than sham animals [29]. Neither the maintained baseline Ca^{2+} transient nor the augmented response to β-AR stimulation are consistent with numerous experimental and clinical studies of symptomatic heart failure e.g. [1,2,31].

Given these considerations the hypothesis examined is that phosphodiesterase 5 inhibition is beneficial in systolic heart failure through restoration of catecholamine responsiveness. As such, the primary aim of the present study was to determine if PDE5 inhibitor treatment, instigated at an advanced disease stage once contractile dysfunction and attenuated catecholamine responsiveness are established, is capable of reversing these effects and conferring a symptom-free survival benefit. The secondary aim of the study was to determine if any contractile, symptom-free survival and catecholamine responsiveness changes were associated with structural (TT) remodeling and the underlying molecular mechanisms of such TT remodeling. The final aim of the study was to determine the underlying mechanisms that contribute to the restoration of catecholamine responsiveness. The major findings are that PDE5 inhibition with tadalafil markedly enhances symptom-free survival, partially reverses contractile dysfunction and restores catecholamine responsiveness *in vivo*. At the cellular level, PDE5 inhibition restored systolic calcium. These changes are associated with a restoration of TT density but β-AR abundance (β_1 and β_2) remained unaltered. However, downstream regulators of catecholamine signalling including GRK2, PKG, PDE2, PDE3, PP1 and PP2A were all differentially regulated by HF and PDE5 inhibition. Our findings also implicate the BAR domain protein amphiphysin II (AmpII *aka* BIN1) as a key driver of the TT changes seen in response to HF and PDE5 inhibitor treatment.

Results

PDE5 inhibition improves symptom-free survival and enhances cardiac contractility in vivo

bioRxiv preprint doi: https://doi.org/10.1101/248187; this version posted January 28, 2019. The copyright holder for this preprint (which was not certified by peer review) is the author/funder. All rights reserved. No reuse allowed without permission.

Of the 27 animals randomly assigned to the tadalafil treatment group, all remained free of signs of heart failure to the completion of the study (day 49, Figure 1A) and one was found dead on day 19 of treatment; notably there were no prior signs of heart failure (including lethargy, dyspnea, weight loss, tussis) and on post-mortem examination the pacing lead was found to have perforated the right ventricular wall and pulmonary congestion was not evident. Conversely, 34 of 42 untreated animals developed signs of heart failure before day 49 and were therefore humanely killed for subsequent *in vitro* experiments. Thus, tadalafil treatment markedly improved symptom-free survival ($p < 0.001$) yielding a Cox's proportional hazard ratio of 0.026 ± 0.03 (95 % CI, 0.003 – 0.19; $p < 0.001$). There was no difference in body weight between the 42 untreated (32.0 ± 1.1 kg) and 26 tadalafil treated animals with weight data (31.6 ± 1.3 kg) and, as such, body weight was not a significant covariate having a hazard ratio of 1.02 ± 0.03 (95 % CI, 0.97 – 1.07; $p = 0.44$). In the tadalafil treated HF animals ($N = 13$) the total plasma tadalafil content determined by mass spectrometry was 269 ± 39 μg/l and plasma tadalafil protein binding measured as 93 ± 0.6 % and thus in good agreement with that in healthy human subjects [32]. Thus, the nadir free tadalafil concentration in HF plasma following 3 weeks of daily dosing (20 mg daily) was 51 ± 8 nmol/l.

We next sought to determine if the increase in symptom-free survival following tadalafil treatment was associated with any changes in cardiac contractility or cardiac dimensions. In line with our previous findings [1,33-35] left ventricular dilatation and free wall thinning were observed following tachypacing (Figure 1B & C). Tadalafil treatment did not reverse left ventricular dilatation but did normalize diastolic wall thickness from its nadir value observed one week after commencement of tadalafil treatment. In sheep the cardiac apex is positioned over the sternum and it is difficult to obtain four chamber apical views in adult animals. Therefore, we used the short axis fractional area change measured at mid papillary muscle level as a surrogate for ejection fraction. Following 4 weeks of tachypacing fractional area change was reduced from pre-pacing values by 43 ± 7 % (Figure 1D) in the untreated group and to the same extent in the tadalafil group before treatment commenced (43 ± 3%, $p < 0.001$; both groups $p < 0.001$ *vs* pre-pacing values). However, tadalafil treatment increased fractional area change such that by the end of the study fractional area change was 16 ± 8 % greater than at 4 weeks ($p < 0.05$) and 35 ± 24 % greater than in the end-stage untreated group ($p < 0.01$). In agreement with the *in vivo* contractility findings and our previous study [1], the amplitude of the

bioRxiv preprint doi: https://doi.org/10.1101/248187; this version posted January 28, 2019. The copyright holder for this preprint (which was not certified by peer review) is the author/funder. All rights reserved. No reuse allowed without permission.

systolic calcium transient was reduced by 66 ± 14 % in HF (Figure 1E, $p < 0.05$). However, following tadalafil treatment the amplitude of the systolic calcium transient was 132 ± 32 % of control values ($p = 0.49$) and therefore was restored to a greater extent than *in vivo* contractility.

Whilst tadalafil treatment augmented cardiac contractility, improved symptom-free survival and systolic calcium, the additive effects of tadalafil treatment on blood pressure were minimal. Previously we have reported that systolic, diastolic and mean blood pressure decrease in HF [36]; an observation repeated here (Table 1). However, tadalafil treatment had no further effect on blood pressure which was indistinguishable from both the 4 week tachypaced and heart failure groups. Thus, the changes in cardiac function associated with tadalafil treatment are not due to changes in peripheral blood pressure.

PDE5 inhibition restores the inotropic and chronotropic response to catecholamine stimulation

Since HF is associated with a reduced responsiveness to β-adrenergic stimulation [1,33] and impaired catecholamine responses are associated with reduced survival in HF patients [37] we next determined if the improved symptom-free survival following chronic tadalafil treatment was also associated with restoration of catecholamine responsiveness. We first examined cardiac contractile responses to intravenous infusion of the exogenous β-adrenergic agonist dobutamine. Whilst left ventricular fractional area change in dobutamine was attenuated in tadalafil treated animals compared to pre-pacing values it was greater than in both untreated animals following 4 weeks of tachypacing and when signs of (end stage) HF were present (Figure 1F, $p < 0.001$). In paired samples (pre-pacing, 4 weeks and tadalafil treated), the absolute fractional area changes (Figure 1F) were reflected in a greater response to dobutamine infusion after tadalafil treatment than after 4 weeks of tachypacing (Figure 1G) indicating that chronic PDE5 inhibition in HF augments catecholamine sensitivity. Furthermore, tadalafil treatment also improved the chronotropic response to dobutamine (Figure 1H). As we have reported previously in a separate study [33], HF attenuated the chronotropic response to dobutamine. In pre-paced animals, 5 μg/kg/min dobutamine shortened RR interval by 36 ± 10 % ($p < 0.01$) yet had no effect

bioRxiv preprint doi: https://doi.org/10.1101/248187; this version posted January 28, 2019. The copyright holder for this preprint (which was not certified by peer review) is the author/funder. All rights reserved. No reuse allowed without permission.

following 4 weeks of tachypacing or in end-stage HF (5.4 ± 8 % and 3.8 ± 2 % respectively). Conversely, at this infusion rate RR interval shortened by 26 ± 6 % in the tadalafil treated animals ($p < 0.01$). To further understand the attenuated chronotropic response, we also investigated the dose-response to dobutamine in a cohort of animals at three time points; pre-pacing, 4 weeks of tachypacing (but before tadalafil treatment commenced) and following 3 weeks of tadalafil treatment (Figure 1I). It is clear that the sensitivity to dobutamine was reduced at 4 weeks of tachypacing and partially restored toward control values following tadalafil treatment. Assuming that the maximal achievable heart rate is equal to that in pre-paced animals treated with 10 $\mu g.kg^{-1}.min^{-1}$ dobutamine, the calculated EC50 concentration of dobutamine is 3.6, 34.4 and 10.7 $\mu g.kg^{-1}.min^{-1}$ in the pre-pacing, 4 weeks tachypaced and tadalafil treated groups respectively ($p < 0.005$). In addition to improving several *in vivo* measures of cardiac function and catecholamine sensitivity, chronic PDE5 inhibition also normalized the tachypacing induced increases in NPPB (B-type natriuretic peptide) mRNA (Figure 2A). Thus, tadalafil treatment at least partially restores both the inotropic and chronotropic response to catecholamines that are lost in HF and reverses increases in mRNA abundance of the widely accepted marker of HF, B-type natriuretic peptide.

The impact of PDE5 inhibition on regulators of cGMP and the β-adrenergic signalling cascade

There was no change in the abundance of PDE5A mRNA (Figure 2B) or cGMP levels in myocardial homogenates (Figure 2C) in HF or following tadalafil treatment. Whilst unaltered PDE5 mRNA levels in HF have been reported previously [29,38], the unchanged myocardial cGMP content following tadalafil treatment was initially surprising. However, examining known regulators of cGMP in HF and following tadalafil treatment we found an increase in total, monomeric (75 kDa) and dimerized (150 kDa) PKG (Figure 2D). Total and 75 kDa PKG abundances were not different between the 4-week paced, HF and tadalafil groups. However, for the 150 kDa dimer of PKG, abundance was greater in the tadalafil group compared to the 4-week paced group and tended to an increase when compared to the HF group ($p = 0.053$). Moreover, tadalafil treatment augmented the abundance of the cGMP hydrolyzing phosphodiesterases PDE2 and PDE3 (Figure 2E & F). Thus, the increased abundance of PKG, through inhibition of sGC [39] and

bioRxiv preprint doi: https://doi.org/10.1101/248187; this version posted January 28, 2019. The copyright holder for this preprint (which was not certified by peer review) is the author/funder. All rights reserved. No reuse allowed without permission.

stimulation of PDE5 [15], coupled with elevated levels of the cGMP hydrolyzing PDEs 2 & 3 provide a plausible explanation for the unchanged myocardial cGMP content despite chronic tadalafil treatment.

In the next experiments we sought to elucidate the impact of chronic PDE5 inhibition in HF on key regulators of catecholamine signalling in the heart. We found no difference in β_1 or β_2 adrenergic receptor abundance in whole heart homogenates following four weeks of tachypacing, in HF or following tadalafil treatment (Figures 3A & B). In agreement with our previous findings [1], in HF the protein abundance of G protein coupled receptor kinase GRK2 and protein phosphatases PP1 and PP2A was increased (Figure 3C-E). The increase in GRK2, PP1 and PP2A was established by 4 weeks of tachypacing, reaffirming adrenergic dysfunction is established prior to PDE5 inhibitor treatment in this study. Importantly, chronic tadalafil treatment resulted in a reduction in protein abundance for each of these regulators of β-adrenergic signalling to either the same level (GRK2, PP1) or lower (PP2A) than in control hearts thus mechanistically linking PDE5 inhibition with the enhanced catecholamine responses noted *in vivo*.

PDE5 inhibition restores the transverse tubule network in heart failure

Since the β_1-AR and β_2-AR are functionally distributed on the TT membrane and surface sarcolemma [5,7] we sought to determine if the restored response to the β-AR agonist dobutamine following tadalafil treatment was associated with changes in TT density or organisation in ventricular myocytes (Figure 4A). To quantify changes in TT density we have adopted two approaches; i) determination of the distance 50 % of voxels (3 dimensional pixels) are from their nearest membrane (TT or surface membrane) in all three imaging planes, termed 'half-distance' [8,34] (Figure 4A.b.) and, ii) determination of the fractional area of the cytosol occupied by TT's in the imaging plane, termed 'fractional area' [8,34]. In agreement with our previous work [8] and others e.g. [9,10,40] heart failure resulted in a decrease in ventricular TT density of 19 ± 5 % measured using the half distance (Figure 2B; $p < 0.001$) and 26 ± 5 % using fractional area methodologies (Figure 4C; $p < 0.001$). Importantly, these changes in TT density had occurred by 4 weeks of tachypacing and therefore the TT density reduction observed in HF was established before commencement of tadalafil treatment (Figure 4B-C). Following 3 weeks of tadalafil treatment, with continued tachypacing, there was a complete

bioRxiv preprint doi: https://doi.org/10.1101/248187; this version posted January 28, 2019. The copyright holder for this preprint (which was not certified by peer review) is the author/funder. All rights reserved. No reuse allowed without permission.

restoration of TT density back to control levels (half-distance: control, 0.377 ± 0.01 μm; tadalafil, 0.369 ± 0.001 μm; fractional area: control, 0.198 ± 0.01; tadalafil, 0.231 ± 0.01).

Despite TT density being fully restored following tadalafil treatment, closer inspection of the skeletonized images (Figure 4A.c.) shows that the TTs are less organized in the tadalafil treated animals than in control myocytes. In control cells TTs are predominantly organized perpendicular to the long axis of the cell (Figure 4D) having a transverse (perpendicularly arranged) to longitudinal (horizontally arranged) ratio of 2.4 ± 0.2 (Figure 4E). After 4 weeks of tachypacing, in end-stage heart failure and following tadalafil treatment TTs are nearly equally oriented longitudinally and transversely (4 weeks, 1.1 ± 0.1; heart failure, 1.0 ± 0.1; tadalafil 1.2 ± 0.1; all $p < 0.001$ versus control). Thus, the restoration of TT density following tadalafil treatment is not matched by normalization of their orientation.

Potential molecular mechanisms responsible for changes in TT density in heart failure and reversal by PDE5i treatment

Although the control of TT turnover remains poorly understood we next sought to identify potential molecular mechanisms responsible for the restoration of TTs following tadalafil treatment. We examined protein abundance of four putative regulators of TT turnover AmpII (BIN1), junctophilin 2 (JPH2), titin capping protein (TCAP) and myotubularin 1 (MTM1). Of these, JPH2 (Figure 5A) and TCAP (Figure 5B) showed no change in abundance with disease duration or tadalafil treatment whereas MTM1 abundance was increased equally above control in the 4 week tachypaced, HF and tadalafil treated animals (Figure 5C, all $p < 0.05$). Conversely, AmpII protein abundance was reduced from control levels in both the 4 week tachypaced and HF groups where TT density is reduced (Figure 5D.a; $p < 0.05$) and restored to control levels in the tadalafil treated group in line with the restoration of TTs. Moreover, AmpII abundance was also greater in the tadalafil group than both the 4 week tachypaced and HF groups ($p < 0.05$). The relationship between TT density and AmpII protein abundance is examined in Figure 5D.b-c. As we have shown previously [8], TT density is correlated with AmpII protein abundance during the development of HF and following treatment with tadalafil ($p < 0.05$).

bioRxiv preprint doi: https://doi.org/10.1101/248187; this version posted January 28, 2019. The copyright holder for this preprint (which was not certified by peer review) is the author/funder. All rights reserved. No reuse allowed without permission.

Whilst our present data (e.g. Figure 5D) and previous studies [8,41] have shown a correlation between AmpII abundance and TT density, there remains some uncertainty over which isoforms of AmpII (BIN1) are expressed in cardiac muscle and drive the formation of TTs in cardiac myocytes. We therefore sought firstly to determine which AmpII isoforms are present within the ovine myocardium. Using RT-PCR approaches and amplifying the variably expressed regions between exons 6 and 18 of AmpII we identified 3 major amplicons in the ovine myocardium (Fig 6A). From amplicon size and subsequent sequence verification we identified the 'skeletal', exon 11 containing v8 isoform as the major AmpII isoform expressed in the myocardium with lower levels of expression of v4 and v10 isoforms. By investigating the role of variant 8 AmpII overexpression in NRVMs and iPSC CMs we sought to establish if the augmented AmpII protein abundance provides a mechanism for the increase in TT density following tadalafil treatment. Importantly, and in contrast to the heterozyous knockout model used by Hong *et al* [42], both cell types lack TTs. Both non-transfected and mKate2 fluorescent protein transfected NRVMs have low endogenous AmpII protein abundance whereas AmpII-AC-mKate2 transfection increased AmpII protein abundance 4.6 ± 0.3-fold (Figure 6B, $p < 0.05$). When transfected NRVMs were imaged confocally (Figure 6C), those that were transfected with the mKate2 control vector exhibited diffuse cytosolic and nuclear fluorescence. Conversely, cells transfected with the AmpII-AC-mKate2 vector exhibited widespread intracellular fluorescence in the form of an inter-connected network. To determine if the AmpII driven network formed tubules connected to the surface sarcolemma cells were superfused with the extracellular fluorescent marker Oregon Green 488N. It is clear from Figure 6C that Oregon Green 488N enters the cell and co-localises with mKate2 fluorescence indicating i) that AmpII forms tubular structures and, ii) these are patent at and connected to the cell surface. On average 97.9 ± 2.1 % cells transfected with AmpII-AC-mKate2 developed a tubular network compared to no tubules in non-transfected or cells transfected with the mKate2 control vector (Figure 6D, $p < 0.001$). The summary data of Figure 6E demonstrates that AmpII-C-mKate2 expression in NRVMs lead to a robust increase in the fractional area of cells occupied by TTs (59 ± 3 fold, $p < 0.001$). Finally, we also confirmed that AmpII was capable of driving *de novo* tubule formation in human iPSC CMs and that these cells also normally lack a discernible tubular network (Figure 6F -H).

bioRxiv preprint doi: https://doi.org/10.1101/248187; this version posted January 28, 2019. The copyright holder for this preprint (which was not certified by peer review) is the author/funder. All rights reserved. No reuse allowed without permission.

Discussion

The main findings of the present study investigating the impact of chronic PDE5 inhibition on cardiac function and structure in heart failure are fourfold: i) PDE5 inhibition prevents the development of the signs of heart failure; ii) PDE5 inhibition restores systolic calcium and catecholamine responsiveness; iii) t-tubule density is reduced in heart failure and fully restored to control levels by PDE5 inhibition and, iv) changes in expression of the putative t-tubule regulator AmpII are correlated with changes in t-tubule density and AmpII drives de novo tubule formation in ventricular myocytes. Importantly, in this study we demonstrate that PDE5 inhibition *reverses* rather than *prevents* the heart failure dependent changes in cellular structure and catecholamine responsiveness as both the reduction in TT density and loss of catecholamine responsiveness are already present before PDE5 inhibition is commenced.

PDE5 inhibition mediated reverse remodeling in heart failure.

This study shows a dramatic impact of PDE5 inhibition on symptom free survival that is effective once advanced cardiac dysfunction has developed before PDE5 inhibition commences. The observed symptom free survival effects are also reflected by normalization of B-type natriuretic peptide mRNA levels within the myocardium. The delayed administration of PDE5 inhibition used here distinguishes this study from the majority of previous studies investigating PDE5 inhibition in HF where treatment was initiated simultaneously with, or prior to, disease initiation [22-27]. Additionally, where earlier studies have implemented delayed PDE5 inhibitor treatment, these appear to have been at a far less advanced stage of HF than in this study based on contractility measurements or the response to catecholamine stimulation [28-30,38]. Thus, this study adds to a growing weight of evidence on the effectiveness of PDE5 inhibition in treating systolic HF and demonstrates reversal of key elements of the disease process that are evident when cardiac dysfunction is at an advanced stage.

Whilst changes in B-type natriuretic peptide mRNA are observed, the PDE5 inhibition mediated effects on HF progression occur in the absence of changes in PDE5A mRNA and cGMP levels within the myocardium. Previous studies have also noted no change in PDE5A abundance in preclinical HF models [29,38] and Hiemstra *et al*, using a porcine

bioRxiv preprint doi: https://doi.org/10.1101/248187; this version posted January 28, 2019. The copyright holder for this preprint (which was not certified by peer review) is the author/funder. All rights reserved. No reuse allowed without permission.

model, reported no change in myocardial cGMP content following tadalafil treatment [38]. In the present study we investigated potential mechanisms that could explain the lack of change in the global cGMP content of the myocardium and found that PKG (monomer, dimer and total levels) and the cGMP hydrolyzing phosphodiesterases PDE2 and PDE3 were augmented following tadalafil treatment. We suggest therefore that the changes in PKG, PDE2 and PDE3 may underlie the lack of a global change in cGMP, yet, there may still remain sub-cellularly restricted pools of elevated cGMP that may influence distinct signalling pathways and underpin the inotropic, chronotropic and 'survival' effects seen with tadalafil treatment.

PDE5 inhibition in heart failure: effects on cardiac function and catecholamine responsiveness.

The first consideration of the effects of tadalafil treatment in heart failure is that of off-target effects. Tadalafil is structurally distinct from other commonly used PDE5 inhibitors (sildenafil, vardenafil) and shows substantially greater (> 1000 fold) specificity for PDE5 over other PDEs than both sildenafil and vardenafil with the exception of PDE11 where the selectivity ratio (PDE5 IC_{50} : PDE11 IC_{50}) is between 7.1 and 40 [43-46]. However, the absence of PDE11 in cardiac myocytes [47] together with the lack of any obvious neurological disturbance or myalgia (PDE11 dependent side-effects) would suggest that despite the plasma concentration of tadalafil used (~ 50 nmol/l) causing complete inhibition of PDE5 (IC_{50} range 0.94 – 9.4 nmol/l) [43,48], the approximate 40 %, inhibition of PDE11 is not underpinning the cardioprotective effects observed in the present study. The development of PDE11 specific antagonists or use of lower doses of tadalafil in future studies would enable this to be conclusively determined.

The main observation in the present study is that the profound symptom-free survival benefit of tadalafil treatment was demonstrated when significant cardiac dysfunction was already present. Of the previous studies examining the effects of PDE5 inhibition in heart disease few have objectively assessed the impact of PDE5 inhibition on development (survival) of left-sided heart failure [27]. However, in that study sildenafil treatment was commenced at the time of disease initiation and it is therefore impossible to conclude whether PDE5 inhibition is beneficial once advanced cardiac disease has been established. Moreover, whilst the development of heart failure in aortic-banded

bioRxiv preprint doi: https://doi.org/10.1101/248187; this version posted January 28, 2019. The copyright holder for this preprint (which was not certified by peer review) is the author/funder. All rights reserved. No reuse allowed without permission.

rats was reduced by sildenafil treatment [27] the magnitude of the effect was considerably less than that observed here following tadalafil treatment. Further work is therefore required to determine if the survival benefits are specific to tadalafil or are a PDE5 inhibitor class effect.

In those studies where PDE5 inhibition has been started at varying time points following disease initiation there is indeed evidence of attenuated deterioration in function or some reversal of extant dysfunction [28,30,49,50]. However, in each of these cases symptom-free survival and catecholamine response data are absent. Conversely, in those studies where the systolic calcium transient or adrenergic responsiveness has been measured they are either maintained [29] or augmented [38] in the 'heart failure' groups suggesting that the disease stage in these particular studies is relatively early. In comparison, the present study, using a large animal model of tacyhcardic end-stage heart failure, demonstrates a dramatic increase in symptom-free survival where contractile and adrenergic dysfunction are established before the onset of PDE5 inhibitor treatment. Furthermore, both the contractile dysfunction and attenuated catecholamine response are at least partially reversed by PDE5 inhibitor treatment. A similar restoration of catecholamine reserve in heart failure has been observed experimentally following cardiac resynchronization therapy and suggested to confer improvements in systolic function and long-term survival to this patient group [51].

In the present study we have investigated the potential mechanisms underpinning the restoration of catecholamine responsiveness following PDE5 inhibition. Whilst we found no change in β_1 or β_2 adrenergic receptor density in HF or following tadalafil treatment it remains possible that the restoration of TT density with tadalafil treatment is important in directing the sub-cellular aspects β-receptor signalling and thence augmenting cardiac contractility [5,52]. However, concordant with the restoration of catecholamine sensitivity [1] we observed tadalafil dependent decreases in GRK2, PP1 and PP2A protein abundance which would increase cAMP levels [53] and enhance target phosphorylation including sites on myofilament proteins, phospholamban and the L-type Ca^{2+} channel [54-56].

PDE5 inhibition in heart failure: effects on cardiac cellular structure.

bioRxiv preprint doi: https://doi.org/10.1101/248187; this version posted January 28, 2019. The copyright holder for this preprint (which was not certified by peer review) is the author/funder. All rights reserved. No reuse allowed without permission.

Increasing evidence implicates a reduction in TT density as a major factor contributing to cardiac dysfunction in diverse cardiac diseases [8-10,22,34,40,57-59]. In the present study, we also note a decrease in TT density in HF and importantly that this is fully reversed by PDE5 inhibitor treatment. Our findings extend the earlier studies of Huang *et al* [27] whereby sildenafil treatment commenced concurrently with aortic-banding prevented TT loss and Xie *et al* [22] where delayed sildenafil treatment partially restored right ventricular TT density in a pulmonary artery hypertension model; although the incomplete recovery of TTs therein may reflect the shorter treatment duration (2 weeks), drug choice (sildenafil) or chamber (right versus left) wall strain differences [60-62].

Whilst tadalafil treatment restores TT density, the TTs in this group are equally distributed in the transverse and longitudinal orientations, rather than predominantly transverse orientation seen in control hearts. Previous studies have noted plasticity in TTs and their ability to be restored to varying extents following interventions to reverse HF [27,62-64] although these have not investigated TT orientation in the various intervention arms. Here, we sought to determine if changes in TT density in HF and following tadalafil treatment are correlated with changes in the abundance of proteins implicated in TT biogenesis in striated muscle [65-67]. Of the putative candidate proteins only one, AmpII, correlates with TT density changes in HF and following tadalafil treatment. AmpII (BIN1) is known to be involved in TT biogenesis in skeletal muscle [68] and in cardiac muscle protein abundance is reduced in HF [8,41,63]. Using siRNA gene silencing in cultured adult ventricular myocytes we have shown that AmpII is required for cardiac TT maintenance [8] and Hong *et al* [42,69] and more recently, De La Mata *et al* [70] demonstrated the importance of BIN1 (AmpII) in delivery of L-type Ca channels to TT membranes and TT membrane folding. In the present study, we extend this earlier work and show that AmpII is capable of driving the *de novo* formation of tubule like structures in both NRVMs and iPSC CMs; model cell types that lack TTs. Importantly, co-labelling with extracellular dye shows that the AmpII driven tubules are patent at the cell surface. Thus, an emerging body of work highlights the importance of AmpII in the TT biology in the heart and future studies will be required to define the functional significance of AmpII driven TT formation.

bioRxiv preprint doi: https://doi.org/10.1101/248187; this version posted January 28, 2019. The copyright holder for this preprint (which was not certified by peer review) is the author/funder. All rights reserved. No reuse allowed without permission.

Moreover, and in stark contrast to the work of Hong *et al* using the mouse [42], we also demonstrate that exon 11 (previously known as exon 10 [71]) containing variants 8 and 4 of AmpII (BIN1) are expressed within the sheep myocardium with variant 8 mRNA being the dominantly expressed isoform and that variant 8 is capable of inducing *de novo* tubulation in cardiac cells. Further work will be required to elucidate the significance of species differences in AmpII isoform usage and the critical components of AmpII for cardiac muscle TT formation; it may be that, as with chamber differences in TT density, important distinctions exist between laboratory rodents and large mammals including human [8,34,72].

Beyond the correlation between AmpII protein abundance and TT density, we also noted a generalized increase in lipid phosphatase MTM1 protein abundance in the 4 week tachypaced, HF and tadalafil treated animals. In skeletal muscle mutations in MTM1 or altered interaction between MTM1 and a number of binding partners, including AmpII lead to inherited centronuclear myopathies, some of which are associated with cardiomyopathies [73,74]. Furthermore, MTM1 augments AmpII driven membrane tabulation [74] and MTM1 deficiency leads to reductions in skeletal muscle TT density [75,76]. Thus, it is possible the increases in MTM1 protein abundance noted in the present study is a compensatory mechanism to maintain TTs in the face of cardiac pathology. However, whether the increase in MTM1 abundance is responsible for the lateralization of TTs in HF and tadalafil treated animals remains to be determined although addressing this in the iPSC and NRVM model systems would be problematic given the inherent disorder of the AmpII driven tubules in these cell types. Finally, there remain the unanswered questions as to whether, i) TT loss is a cause or consequence of HF and, ii) if tadalafil improves cardiac function and this allows TT density to recover or, tadalafil drives TT recovery and thence improves cardiac function. Irrespective of these potential caveats, the dependence of TT maintenance on AmpII [8] and the demonstration in the present study that AmpII drives *de novo* tubule formation in cardiac myocytes highlights AmpII as a target for future studies. Selectively manipulating AmpII protein abundance in established and evolving cardiac disease states in future studies could resolve this question.

Limitations

bioRxiv preprint doi: https://doi.org/10.1101/248187; this version posted January 28, 2019. The copyright holder for this preprint (which was not certified by peer review) is the author/funder. All rights reserved. No reuse allowed without permission.

There are some limitations to the present study that arise primarily from the lack of suitable reagents exhibiting satisfactory cross-reactivity with sheep. As such, we have been unable to serially assess natriurtetic peptide (BNP or NT-proBNP) levels in plasma to monitor the progression and resolution of HF; however, we do observe a strong up-regulation of myocardial NPPB (BNP) mRNA in HF and normalization in the tadalafil treated animals using a single time point assay in each group of experimental animals. Similarly, we have been unable to determine PDE5A protein abundance and have relied on quantitative PCR based assessments. Whilst our work shows no change in the myocardial cGMP content we cannot rule out the possibility that cGMP is elevated in certain sub-cellular pools and thus mediates the effects of tadalafil treatment that we observe. FRET based sensors may offer some potential to assess sub-cellular cyclic nucleotide pools, their use in sheep would require maintenance of primary cardiac myocytes in extended culture to allow transgene expression and thus significant concerns would arise from cellular de-differentiation and ultrastructural changes that inevitably occur when adult cardiac cells are maintained in culture conditions. A further limitation in the present study arises from the anatomical alignment over the cardiac apex over the sternum in adult sheep and inaccessibility to a suitable imaging window to allow four-chamber apical views for a thorough echocardiographic assessment of ejection fraction and E/A ratios. Furthermore, we have found cardiac conductance catheterization to be of limited use given interference from the pacing lead in the right ventricle. Nevertheless, short axis trans-thoracic imaging is possible and clearly shows marked cardiac dilatation and reduced contractility in HF that is at least partially normalized by tadalafil treatment.

In summary, using a large animal model of end-stage heart failure we have shown that chronic treatment with the PDE5 inhibitor tadalafil leads to a dramatic increase in symptom-free survival. Our data suggests that PDE5 inhibition reverses already established cellular ultra-structural remodeling and impaired catecholamine responses in HF. Given the localization of β-ARs and G-protein coupled regulators of cardiac catecholamine responses across the TT and surface sarcolemma, the recovery of TTs following PDE5 inhibition provides a cellular mechanism for the restoration of

bioRxiv preprint doi: https://doi.org/10.1101/248187; this version posted January 28, 2019. The copyright holder for this preprint (which was not certified by peer review) is the author/funder. All rights reserved. No reuse allowed without permission.

catecholamine reserve in tadalafil treated animals and thence the improvement in symptom-free survival.

bioRxiv preprint doi: https://doi.org/10.1101/248187; this version posted January 28, 2019. The copyright holder for this preprint (which was not certified by peer review) is the author/funder. All rights reserved. No reuse allowed without permission.

Methods

Ethical Approval

All experiments were conducted in accordance with The United Kingdom Animals (Scientific Procedures) Act, 1986 and European Union Directive EU/2010/63. Local ethical approval was obtained from The University of Manchester Animal Welfare and Ethical Review Board. Reporting of animal experiments is in accordance with The ARRIVE guidelines [77].

Ovine heart failure model and drug treatment

HF was induced in 69 female Welsh Mountain sheep (~ 18 months) by right ventricular tachypacing as described previously [1,8,34-36,78,79]. In brief, anaesthesia was induced and maintained by isoflurane inhalation (1 – 5 % in oxygen). Under aseptic conditions using transvenous approaches a single bipolar endocardial pacing lead was actively fixed to the right ventricular apical endocardium and connected to a cardiac pacemaker (e.g. Medtronic Sensia, Medtronic Inc. USA) and buried subcutaneously in the right pre-scapular region. Peri-operative analgesia (meloxicam, 0.5 mg/kg) and antibiosis (enrofloxacin 5mg/kg or oxytetracycline 20mg/kg) were administered subcutaneously and animals allowed to recover post-operatively for at least 1 week prior to commencement of tachypacing (210 beats per minute; bpm). Animals were monitored at least once daily for onset of clinical signs of heart failure including lethargy, dyspnoea and weight loss. Following 28 days of tachypacing animals (N = 27) were randomly assigned to receive the PDE5i tadalafil. Treated animals were administered 20 mg tadalafil (Cialis; Lilly, Netherlands) orally once daily for a further 3 weeks and tachypacing (210 bpm) was continued throughout the treatment period. The designated endpoint for the study was either the onset of signs of HF (dyspnoea, lethargy, weight loss) or 49 days of tachypacing (21 days tadalafil treatment).

In vivo assessments of cardiac contractility and catecholamine responsiveness

bioRxiv preprint doi: https://doi.org/10.1101/248187; this version posted January 28, 2019. The copyright holder for this preprint (which was not certified by peer review) is the author/funder. All rights reserved. No reuse allowed without permission.

During echocardiographic and electrocardiographic assessments tachypacing was stopped for 15 minutes prior to data acquisition. Following *in vivo* functional assessments tachypacing was continued at 210 bpm.

Cardiac dimensions and contractility were assessed by right para-sternal transthoracic echocardiography (Vivid 7; GE Healthcare, UK) in non-sedated conscious sheep gently restrained in a supine position. Due to the anatomical alignment of the ventricular apex over the sternum in sheep we are unable to obtain satisfactory 4 chamber long axis views and therefore calculate ejection fraction. However, fractional shortening was measured using m-mode imaging at a level proximal to the papillary muscles and fractional area change calculated from short-axis 2d views at the mid-papillary level [33].

Heart rate was determined from a five-lead ECG (Iox, EMKA Technologies, France). The chronotropic response to β-adrenergic stimulation was assessed as described previously [33] by intravenous infusion of dobutamine hydrochloride (0.5 – 20 μg/kg/min) prepared in 0.9 % saline (Baxter, UK) and delivered using an infusion pump (Harvard Apparatus, UK). Heart rate was determined after 5 mins of dobutamine infusion at each dose and then the infusion rate was doubled to a maximum dose of 20 μg/kg/min or until the heart rate reached 240 bpm.

Transverse tubule staining and quantification

Single left ventricular mid-myocardial myocytes were isolated using a collagenase and protease digestion technique as described in detail previously [1,8,34,79]. Briefly, animals were killed by an overdose of pentobarbitone (200 mg/kg intravenously). Heparin (10,000 units) was also used to prevent coagulation. The heart was rapidly excised and left anterior descending coronary artery cannulated and perfused with collagenase (Worthington Type II, 0.1mg/ml) and protease (from *Streptomyces griseus*, 0.02 mg/ml) containing solutions and single myocytes dispersed by gentle trituration in a taurine solution containing (in mmol/l): NaCl, 113; taurine, 50; glucose, 11; HEPES, 10; BDM, 10; KCl, 4; $MgSO_4$, 1.2; Na_2HPO_4, 1.2; $CaCl_2$, 0.1 and BSA, 0.5mg.ml^{-1} (pH 7.34 with NaOH). Changes in intracellular Ca^{2+} concentration were measured using Fura-2 at 37 ^{o}C in cells electrically stimulated at 0.5 Hz as we have described previously [1,35,80].

bioRxiv preprint doi: https://doi.org/10.1101/248187; this version posted January 28, 2019. The copyright holder for this preprint (which was not certified by peer review) is the author/funder. All rights reserved. No reuse allowed without permission.

TT's were visualized by staining with di-4-ANEPPS (4 μmol/l. Invitrogen, UK) as described in detail previously [8,34,72]. Stained myocytes were imaged by confocal microscopy (Leica SP2 or Zeiss 7Live; 488 nm excitation and 505 nm long pass emission settings) at 100 nm XY pixel dimensions and 162 nm Z-step size. Images were deconvolved using the microscope specific derived point spread function (PSF) using Huygens Software (Scientific Volume Imaging, Netherlands)[8,34,72,81]. Following background correction and image thresholding the following quantitative assessments of TT's were calculated: i) TT fractional area derived from binarized images as the pixels occupied by TT's as a fraction of the planar cell area (ImageJ. NIH, USA), ii) the distance 50 % of voxels in the cell are from the nearest membrane (TT or surface sarcolemma), hereafter referred to as the half-distance, was determined using custom algorithms written in IDL (Exelisvis, UK) [8,34,72]. Images were first interpolated to give the same X, Y, Z spacing ('congrid') and then Euclidean distance maps determined ('morph_distance') and, iii) TT orientation was determined from skeletonized binary images as described previously [8,59] using the ImageJ plugin 'Directionality'.

mRNA, protein expression and cGMP content analysis

Changes in protein expression were assessed in samples obtained from the same hearts used for *in vivo* and TT visualization experiments using approaches described in detail previously [1,8,35]. Following cardiac excision, a ~ 1 cm^3 region of the posterior left ventricular free wall was removed and snap frozen and stored in liquid nitrogen until analysis. Whole myocardium homogenates (~ 100 mg starting material) were prepared in RIPA buffer with protease and phosphatase inhibitors (0.1 mg/ml phenylmethanesulphonylfluroide, 100 mmol/l sodium orhtovanadate, 1mg/ml aprotonin, 1mg/ml leupeptin) and protein content determined (DC Protein Assay, BioRad, UK). Proteins were separated by PAGE, transferred to nitrocellulose membranes and protein expression determined using the antibodies and blotting conditions outlined in Table 2. For PKG protein measurements, sample preparation and blots were conducted under non-reducing conditions. Membranes were visualized by chemiluminescence (Syngene, UK) or IR-Dye labeled secondary antibodies (Licor, UK). Previously we determined that the 'classical' housekeeping proteins GAPDH and β-actin have altered expression in various disease states and therefore we normalized

bioRxiv preprint doi: https://doi.org/10.1101/248187; this version posted January 28, 2019. The copyright holder for this preprint (which was not certified by peer review) is the author/funder. All rights reserved. No reuse allowed without permission.

expression of our protein of interest to an internal control (IC) common to each blot *and* total protein transferred to the membrane determined *either* by Ponceau S staining or REVERT total protein stain (Licor, UK). The IC was derived from a single control sheep (which itself was not included in the present study). Blots were repeated in triplicate on separate occasions and data averaged to minimize any effects due to pipetting or protein transfer errors. Full length blots and validation controls are shown in Supplemental Information (Figure S1).

Total RNA was isolated using Trizol reagent, purified using RNAeasy columns (Qiagen, UK) following manufacturers recommendations. RNA yield and integrity were determined using a Nanodrop (ThermoFisher, UK) and TapeStation (Agilent, UK) instruments respectively. 1 µg total RNA (RIN scores > 7.0) was then reverse transcribed using a high capacity RNA to cDNA kit (Applied Biosystems, UK) following manufacturers steps. PDE5A (Oa04859755_m1) and NPPB (Oa04931155_g1) mRNA abundance was determined using Taqman single tube FAM-MGB assays (ThermoFisher, UK) following the manufacturers protocols and normalized to either RPLPO alone (Oa04824512_g1) or TBP (Oa0481075_m1) and YWHAZ (Oa03216375_gH) combined using the $2^{-\Delta\Delta C_t}$ method (Supplemental Information, Figure S2). All qPCR experiments were repeated 3 times and data averaged. For AmpII (BIN1) isoform determination the variably expressed region between exon 6 and exon 18 (Supplemental Information, Figure S3) was assessed using standard PCR approaches using primers (Eurofins, Germany; forward) 5'-TACGAGTCCCTTCAAACCGC, (reverse) 5'-AGTGTCAACGGCTCTTCCAG. Phusion high fidelity DNA polymerase with GC rich buffer was used for hot start PCR amplification (98 °C, 30 sec; 40 cycles; 98°C - 10sec, 62.1 °C - 30 sec, 72 °C - 30 sec; 72 °C - 10 min) and amplicons separated using a Qiaxcel Advanced Separation System using 15 - 3000 bp markers (Qiagen, UK).

Myocardial cGMP content was determined by competitive ELISA (Amersham, UK) following the manufacturers non-acetylation procedure. Tissue was homogenized in 6 % (w/v) trichloracetic acid, centrifuged and the supernatant washed 4 times before lyophilisation under nitrogen at 60 °C and proceeding to the immunoassay.

bioRxiv preprint doi: https://doi.org/10.1101/248187; this version posted January 28, 2019. The copyright holder for this preprint (which was not certified by peer review) is the author/funder. All rights reserved. No reuse allowed without permission.

Isolation of Neonatal Rat Ventricular Myocyte, induced pluripotent stem cell cardiac myocyte culture and AmpII overexpression

Neonatal rat ventricular myocytes (NRVMs) were isolated from 2 day old Wistar rats and plated onto 8 well plates (Ibidi μ-plates; Thistle Scientific UK) at a density of ~ 3 x 10^5 cells/ml in media (containing: DMEM, 68 %, M199, 17 %; normal horse serum, 10 %; fetal bovine serum, 5 %; all Gibco Life Technologies, UK). Fungizone, Penicillin (10,000 units/ml) and streptomycin (10 mg/ml) were added to a final concentration of 1 % and bromodeoxyuridone (100 μmol/l) added to retard fibroblast proliferation. Cells maintained at 37 ^{o}C in a 5 % CO_2 incubator and media changed every 2 – 3 days. In brief, rat pups were killed by cervical dislocation, bodies rinsed in 70 % ethanol and the ventricles rapidly excised and placed in ice cold dissociation buffer (mmol/l: NaCl, 116; HEPES, 20; glucose, 5.6; KCl, 5.4; NaH_2PO_4, 1; $MgSO_4$, 0.83; pH 7.35). Single NRVMs were digested using 0.75 mg/mL collagenase A (Roche, UK) and 1.3 mg/ml pancreatin (Sigma, UK) by gentle stirring (120 rpm, 7 minutes, 37 ^{o}C) and trituration with a 25 ml Stripette. NRVMs (1 – 3 days post isolation) were transiently transfected with either variant 8 of human BIN1 (AmpII) (Origene Inc, USA) cloned into pCMV6-AC-mKate2 entry vector (Origene Inc, USA) or pCMV6-mKate2 as a negative control. Plasmid DNA (6 μg) was mixed (1 : 3 ratio) with transfection reagent (Fugene 6; Promega, UK) in reduced serum media (OptiMEM; Gibco Life Technologies, UK) and cells transfected and maintained in a 5 % CO_2 incubator at 37 ^{o}C for 48 hours prior to visualization using a Nikon A1R$^+$ confocal microscope (excitation, 561 nm; emission 595 ± 50 nm). The density (fractional area) of tubular structures was determined as described above for adult ventricular myocytes.

Human induced pluripotent stem cell derived cardiac myocytes (iPSC CMs) were purchased (Cellular Dynamics International, USA) and stored in liquid nitrogen until use. Cells were thawed, plated (~6 x 10^4 cells/cm^2) and maintained as per the manufacturer's instructions and using the manufacturers supplied media (iCell cardiomyocyte plating and culture media). Media was changed every 2 days. Five days after plating cells were transfected as described for NRVMs. Tubular structures were quantified by determining the fractional area as described above.

Determination of plasma tadalafil concentration and plasma protein binding

bioRxiv preprint doi: https://doi.org/10.1101/248187; this version posted January 28, 2019. The copyright holder for this preprint (which was not certified by peer review) is the author/funder. All rights reserved. No reuse allowed without permission.

Plasma tadalafil concentration (N = 13) was determined by mass spectrometry. Briefly whole blood from chronically treated and tachypaced animals was collected from the jugular vein in to K_2EDTA blood collection tubes (Vacutainer; Becton Dickinson & Co, UK) on the day of euthanasia and stored on ice. Following centrifugation (4000 *g* for 15 minutes, 4 ^{o}C; within 30 minutes of sample collection) plasma was stored in liquid nitrogen until analysis. Tadalafil concentrations were subsequently determined using a liquid chromatography-mass spectrometry method modified from Kim *et al* [82]. Briefly, following metabolite extraction samples were spiked with heavy stable-isotope containing Tadalafil and Sildenafil (Toronto Research Chemicals, Canada). Each sample was analysed using a Selected Reaction Monitoring method on a ThermoFisher Accela UHPLC coupled to a ThermoFisher TSQ Vantage, using transitions described by Kim *et al* [82]. with sample blanks and tadalafil spiked samples analysed periodically to ensure quantitative accuracy. Tadalafil concentration was calculated by comparing the peak area of the endogenous compound to that of its heavy labelled counterpart. Tadalafil plasma protein binding was also determined by mass spectrometry following rapid equilibrium dialysis (ThermoFisher, UK). K_2EDTA plasma samples (100 µl) from tadalafil treated animals were dialysed in to phosphate buffered saline following manufacturers instructions. Following dialysis equal volumes of control plasma or phosphate buffered saline were added respectively to the dialysate and sample plasma prior to mass spectrometry. The percentage plasma protein bound tadalafil was calculated as (dialysate concentration / sample concentration) x 100.

Statistics

Data are presented as mean ± standard error of the mean (SEM) for n observations / N experiments (animals). Where multiple observations (n) have been obtained from the same animal (N) linear mixed modeling (SPSS Statistics. IBM, USA) was performed thus accounting for the nested (clustered) design of the experiment e.g. multiple cellular or molecular observations from the same heart and replicate Western blots. Data were $\log_{10}$ transformed prior to linear mixed modeling [83]. Dose response and echocardiographic experiments were assessed using a linear mixed modelling ('xtmixed'; Stata, StataCorp USA) or one-way analysis of variance with Bonferroni correction for multiple comparisons ('oneway'; Stata, Stacorp USA) as indicated in figure

bioRxiv preprint doi: https://doi.org/10.1101/248187; this version posted January 28, 2019. The copyright holder for this preprint (which was not certified by peer review) is the author/funder. All rights reserved. No reuse allowed without permission.

legends. Survival data and Cox's proportional hazard ratios were also assessed using Stata ('stcox'). Linear regressions were fitted to non-paired data (Fig 5) by simulating 1000 randomly sampled (7 points in each condition without replacement) data subsets and fitting each of these with a linear regression. The mean slope and 95 % confidence limits were then obtained and superimposed on the plotted mean ± SEM data points. All values were considered significant when $p < 0.05$.

Data & Code Availability

The data that support the findings of this study are available from the corresponding author on reasonable request. Similarly, computer code (IDL) used for assessment of TT density are available from the corresponding author on reasonable request.

Acknowledgements

This work was supported by grants from The British Heart Foundation: FS/12/57/29717, CH200004/12801, FS/15/28/31476, FS/10/71/28563, PG/15/70/31724, IG/15/2/31514, FS/09/002/26487, FS/12/34/29565, FS/15/67/32038, FS/10/52/28678 and Medical Research Council: MR/K500823/1, MR/K501211/1. The authors also acknowledge technical support from Medtronic UK. and Oscor Inc. (USA) in the form of high rate pacing patches for pacing devices and adaptors for pacing leads respectively.

Author Contributions

Study Conception & Design: AWT; Supervision: AWT, DAE, KMD; Animal models, in vivo data generation and analysis: ML, AWT, EJR, CMP, GJK, GWPM, LSW, DCH & LKB; mRNA, protein and cGMP studies CERS, EJR, JLC & RFT; Mass spectrometry: SJC & RDU. All authors contributed to manuscript drafting / editing.

Competing Financial Interests

None

Materials & Correspondence

Andrew.W.Trafford@manchester.ac.uk

bioRxiv preprint doi: https://doi.org/10.1101/248187; this version posted January 28, 2019. The copyright holder for this preprint (which was not certified by peer review) is the author/funder. All rights reserved. No reuse allowed without permission.

	Systolic BP (mmHg)	Diastolic BP (mmHg)	Pulse Pressure (mmHg)	Mean (mmHg)
Control (15)	114 ± 3	68 ± 2	56 ± 3	85 ± 2
4 weeks (10)	105 ± 4	62 ± 3 *, §	43 ± 3	80 ± 4
Heart failure (5)	102 ± 5 *, §	57 ± 5 *, §	45 ± 4	72 ± 5 *, §
Tadalafil (5)	97 ± 5 *, §	55 ± 5 *, §	42 ± 4 §	73 ± 4 *, §

Table 1. The influence of heart failure and tadalafil treatment on blood pressure measured by tail cuff plethysmography.
Summary blood pressure data (mean ± standard error). Values in brackets denote number of animals in each condition. *, denotes $p < 0.05$ vs. control (One way ANOVA with SNK correction for multiple comparisons). §, denotes $P < 0.05$ vs. control (paired t-test).

bioRxiv preprint doi: https://doi.org/10.1101/248187; this version posted January 28, 2019. The copyright holder for this preprint (which was not certified by peer review) is the author/funder. All rights reserved. No reuse allowed without permission.

	Protein loaded (µg)	Blocker	Primary Antibody	Secondary antibody	Detection
Amphiphysin II (AmpII)	40µg	5% BSA	1:200, sc-23918 (Santa Cruz Biotechnology)	1:40,000 HRP conjugated anti-mouse	Chemi-luminescence
Junctophilin2 (JPH2)	10µg	SEABLOCK	1:1,000, sc-51313 (Santa Cruz Biotechnology)	1:40,000 HRP conjugated anti-goat	Chemi-luminescence
Telethonin (TCAP)	20µg	5% Milk	1:500, ab133646 (Abcam)	1:40,000 HRP conjugated anti-rabbit	Chemi-luminescence
Myotubularin (MTM1)	40µg	10% Milk	1:500, ab103626 (Abcam)	1:40,000 HRP conjugated anti-rabbit	Chemi-luminescence
β_1-adrenergic receptor (β_1-AR)	20µg	10% Milk	1:2,000, sc-568 (Santa Cruz Biotechnology)	1:20,000 IRDye 800CW anti-rabbit	Fluorescent
β_2-adrenergic receptor (β_2-AR)	30µg	10% Milk	1:1000, ab137494 (Abcam)	1:20,000 IRDye 800CW anti-rabbit	Fluorescent
G protein receptor kinase 2 (GRK2)	20µg	10% Milk	1:1,000, sc-562 (Santa Cruz Biotechnology)	1:20,000 IRDye 800CW anti-rabbit	Fluorescent
Protein phosphatase 1 (PP1)	20µg	10% Milk	1:1,000, sc-7482 (Santa Cruz Biotechnology)	1:20,000 IRDye 800CW anti-mouse	Fluorescent
Protein phosphatase 2a (PP2a)	20µg	10% Milk	1:1500, sc-80665 (Santa Cruz Biotechnology)	1:20,000 IRDye 800CW anti-mouse	Fluorescent
Protein kinase G (PKG)	20µg	10% Milk	1:1,000, ADI-KAP-PK005 (Enzo Life Sciences)	1:10,000 IRDye 800CW anti-rabbit	Fluorescent
PDE2A	20µg	5% Milk	1:750 ab55555 (Abcam)	1:10,000 IRDye 800CW anti-mouse	Fluorescent
PDE3A	20 µg	SuperBlock	1:1,000, sc-11830 (Santa Cruz Biotechnology)	1:5,000 HRP conjugated anti-goat	Chemi-luminescence
β-actin (loading ctrl)	-	-	1: 5,000, sc-47778 (Santa Cruz Biotechnology)	1:40,000 HRP conjugated anti-mouse	-

Table 2. Blotting conditions for selected proteins

bioRxiv preprint doi: https://doi.org/10.1101/248187; this version posted January 28, 2019. The copyright holder for this preprint (which was not certified by peer review) is the author/funder. All rights reserved. No reuse allowed without permission.

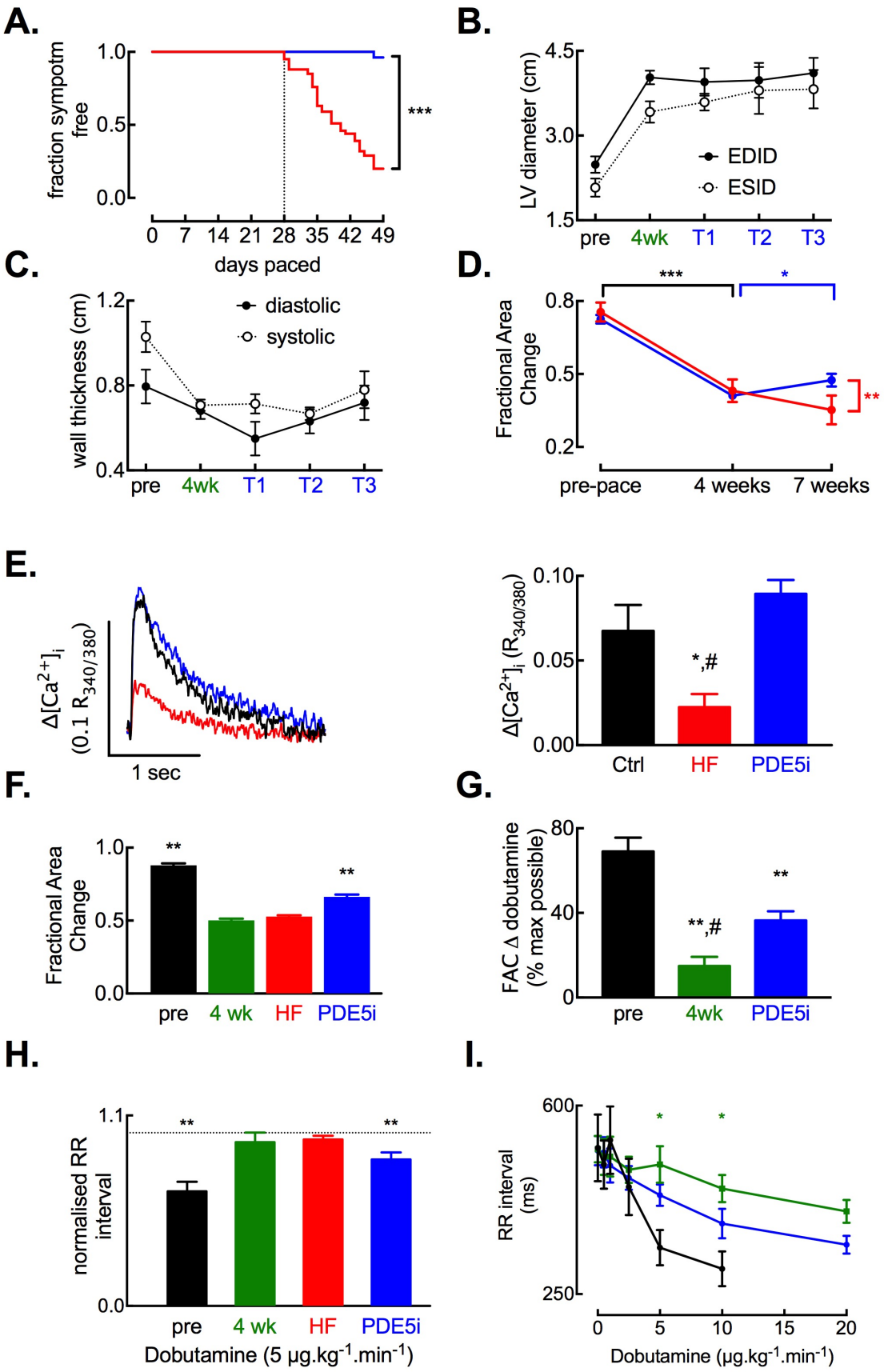

Figure 1

bioRxiv preprint doi: https://doi.org/10.1101/248187; this version posted January 28, 2019. The copyright holder for this preprint (which was not certified by peer review) is the author/funder. All rights reserved. No reuse allowed without permission.

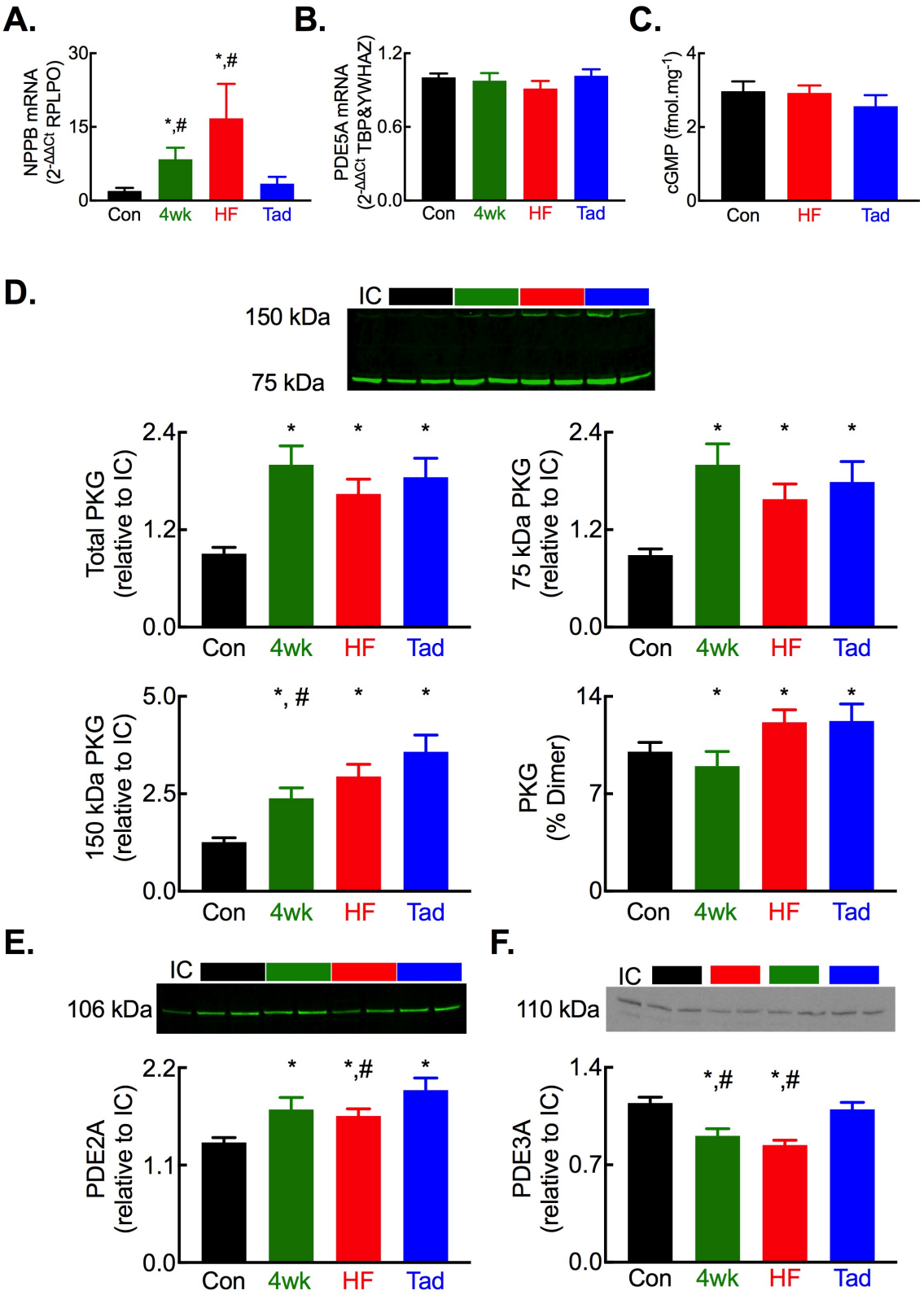

Figure 2

bioRxiv preprint doi: https://doi.org/10.1101/248187; this version posted January 28, 2019. The copyright holder for this preprint (which was not certified by peer review) is the author/funder. All rights reserved. No reuse allowed without permission.

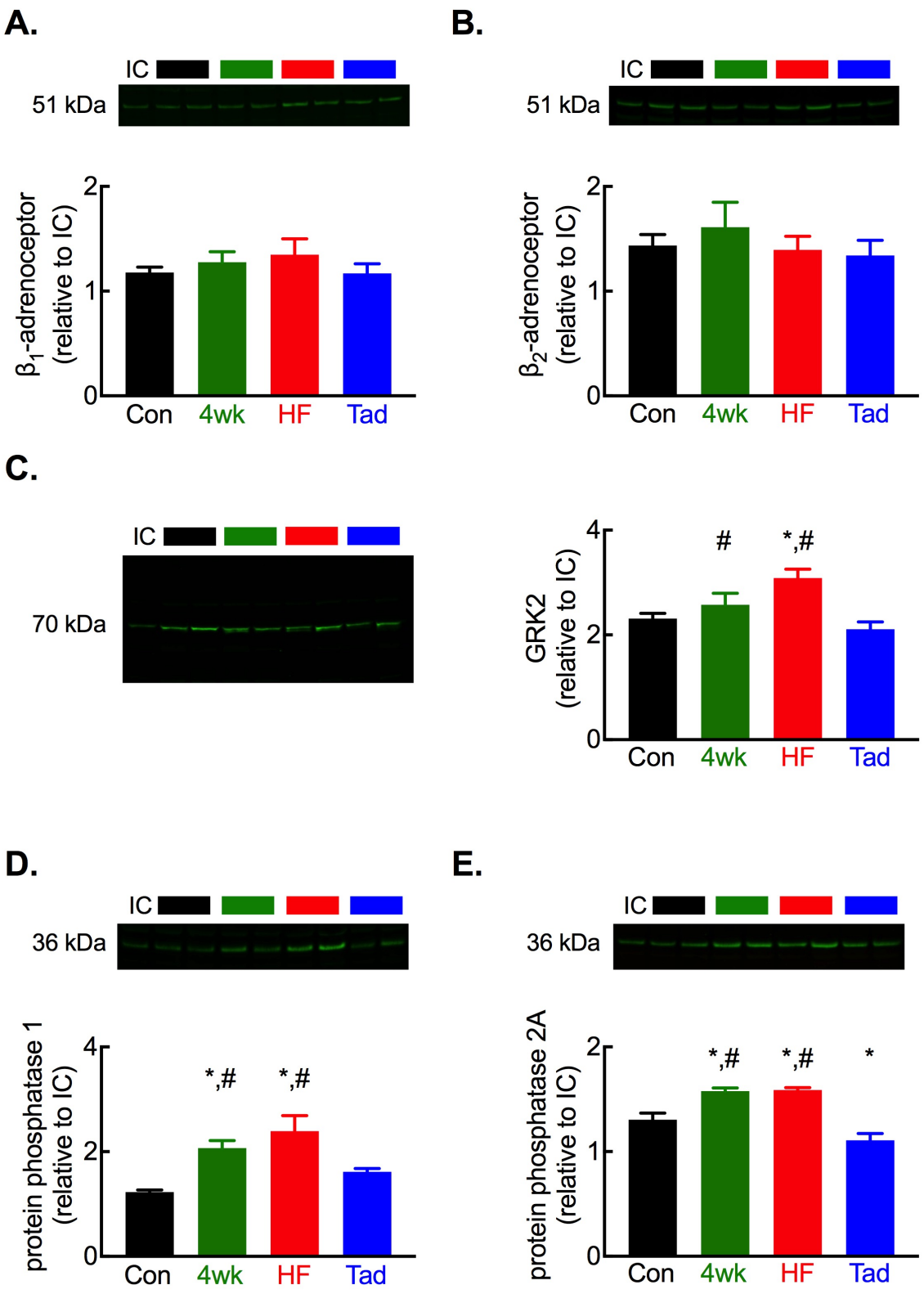

Figure 3

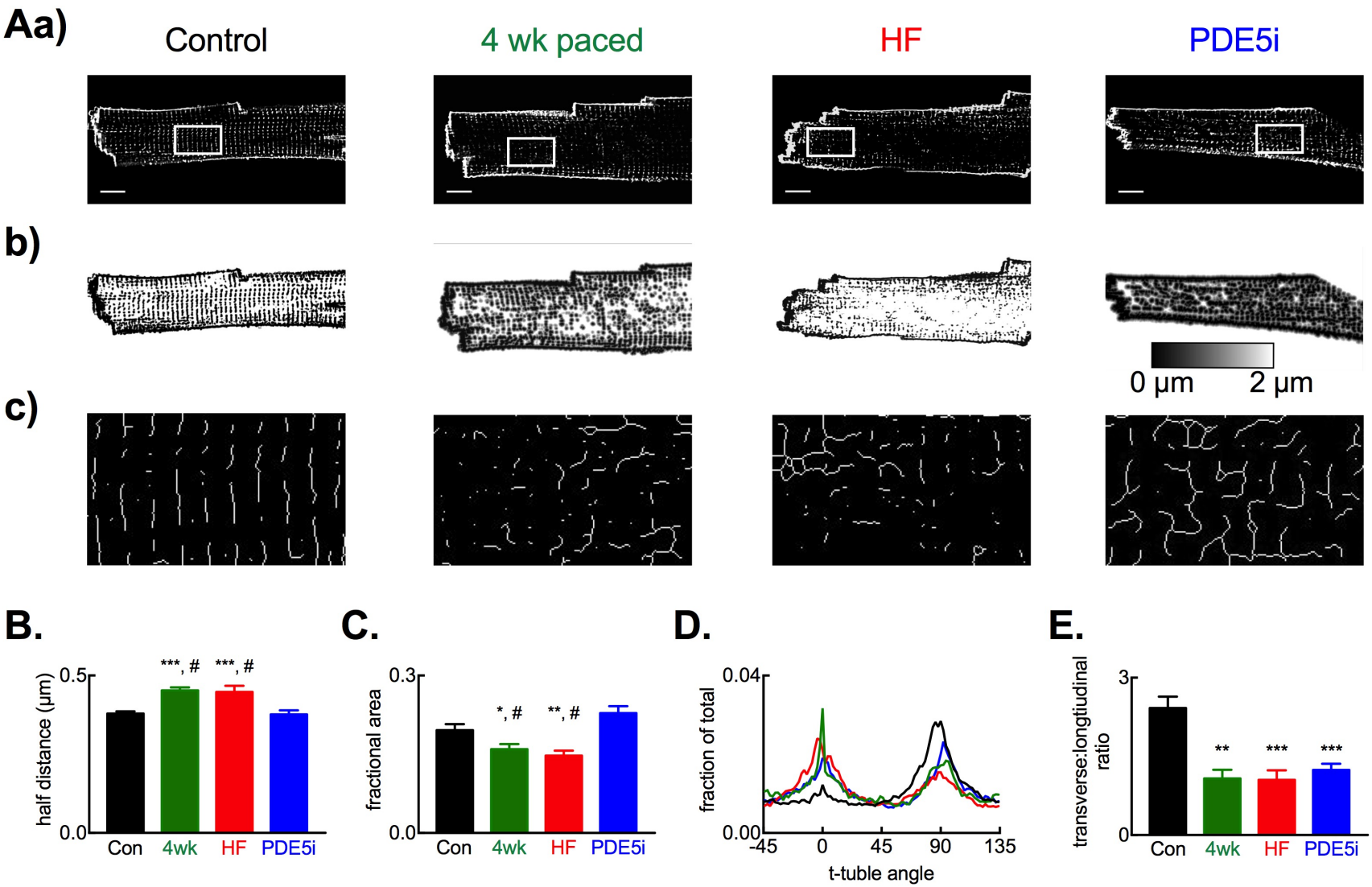
Aa)
Control
4 wk paced
HF
PDE5i
b)
0 µm
2 µm
c)
B.
half distance (µm)
0.5
0.0
***, #
***, #
Con
4wk
HF
PDE5i
C.
fractional area
0.3
0.0
*, #
**, #
Con
4wk
HF
PDE5i
D.
fraction of total
0.04
0.00
-45
0
45
90
135
t-tuble angle
E.
transverse:longtiudinal ratio
3
0
**
***
***
Con
4wk
HF
PDE5i

Figure 4

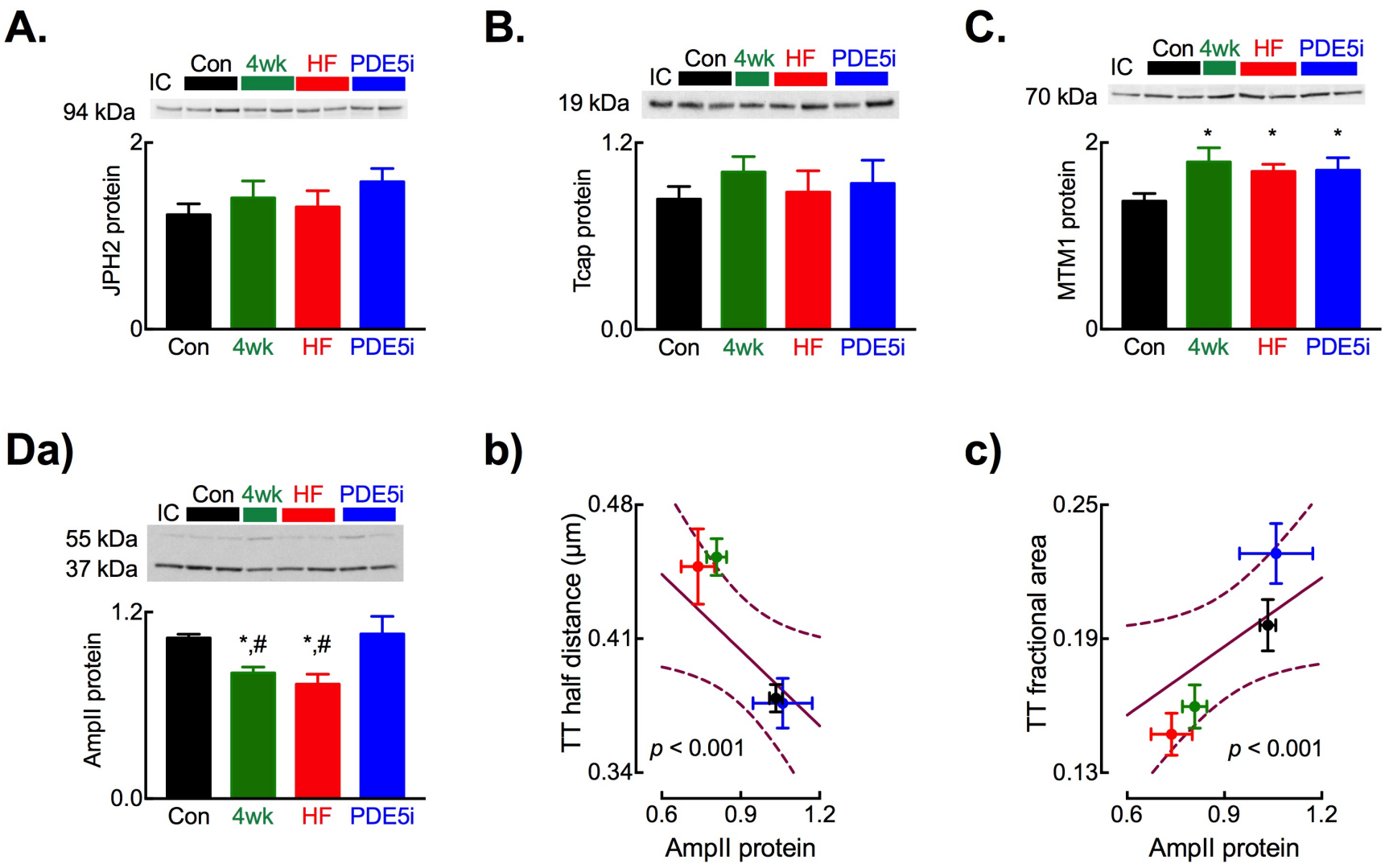
A.
IC
Con 4wk HF PDE5i
94 kDa
JPH2 protein
2
0
Con 4wk HF PDE5i
B.
IC
Con 4wk HF PDE5i
19 kDa
Tcap protein
1.2
0.0
Con 4wk HF PDE5i
C.
IC
Con 4wk HF PDE5i
70 kDa
MTM1 protein
2
0
*
*
*
Con 4wk HF PDE5i
Da)
IC
Con 4wk HF PDE5i
55 kDa
37 kDa
AmpII protein
1.2
0.0
*,#
*,#
Con 4wk HF PDE5i
b)
TT half distance (µm)
0.48
0.41
0.34
p < 0.001
0.6
0.9
1.2
AmpII protein
c)
TT fractional area
0.25
0.19
0.13
p < 0.001
0.6
0.9
1.2
AmpII protein

Figure 5

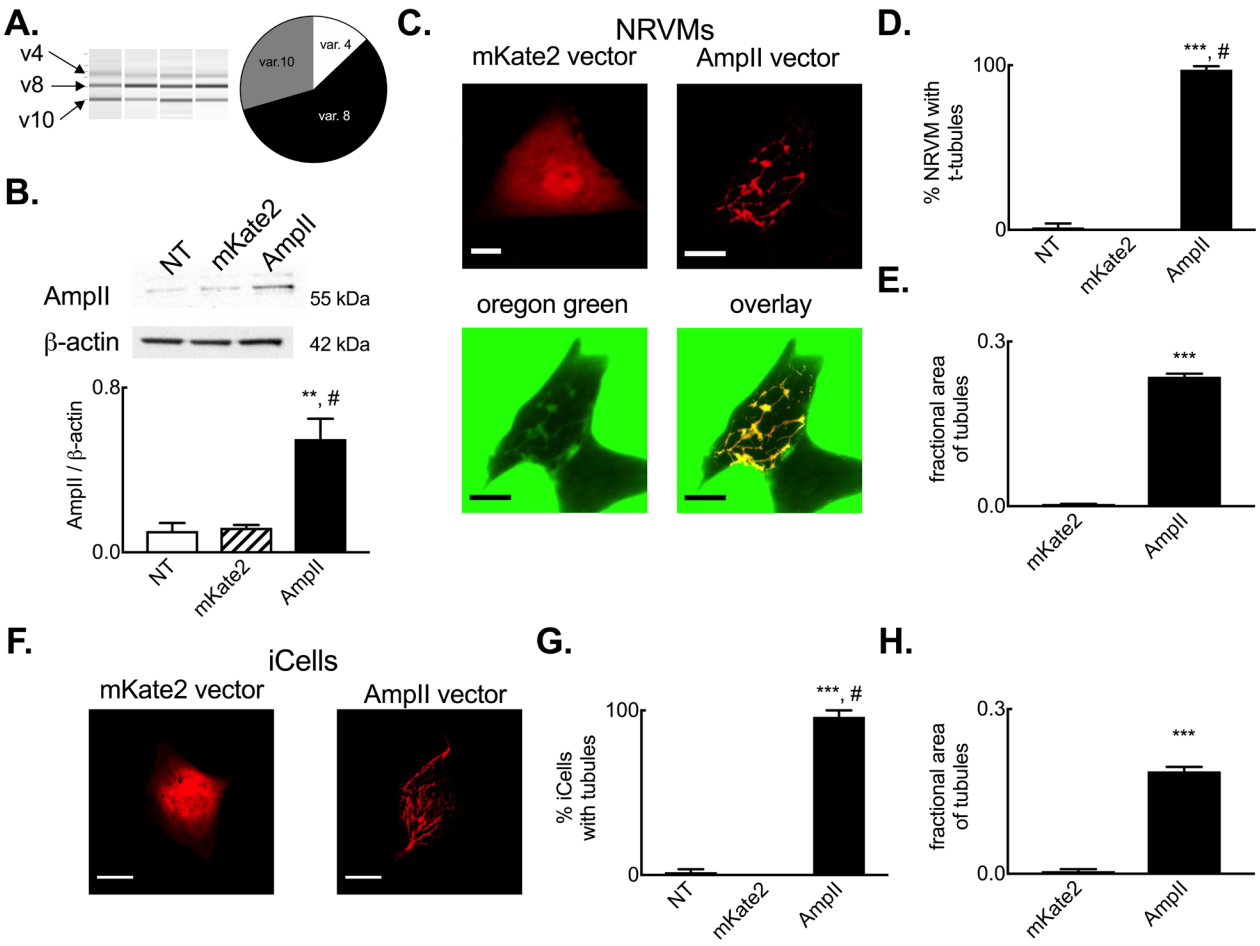
A.
v4
v8
v10
var.10
var. 4
var. 8
B.
NT
mKate2
AmpII
AmpII
55 kDa
β-actin
42 kDa
AmpII / β-actin
0.8
0.0
**, #
NT
mKate2
AmpII
C.
NRVMs
mKate2 vector
AmpII vector
oregon green
overlay
D.
% NRVM with t-tubules
100
0
***, #
NT
mKate2
AmpII
E.
fractional area of tubules
0.3
0.0
***
mKate2
AmpII
F.
iCells
mKate2 vector
AmpII vector
G.
% iCells with tubules
100
0
***, #
NT
mKate2
AmpII
H.
fractional area of tubules
0.3
0.0
***
mKate2
AmpII

Figure 6

bioRxiv preprint doi: https://doi.org/10.1101/248187; this version posted January 28, 2019. The copyright holder for this preprint (which was not certified by peer review) is the author/funder. All rights reserved. No reuse allowed without permission.

Figure 1. Improved symptom-free survival and functional consequences of tadalafil treatment in heart failure.

A. Survival plot showing fraction of animals free from signs of heart failure (*N* = HF, 42; tadalafil, 27). Tadalafil treatment commenced 28 days after tachypacing (dashed line): ***, denotes $p < 0.001$ (by Cox regression-based test). **B.** Changes in left ventricular dimensions with tachypacing and response to tadalafil treatment (*N* = 4 – 6 each time point). **C.** Changes in left ventricular free wall thickness in response to tachypacing and tadalafil treatment (*N* = 4 – 6 each time point). **D.** Echocardiographic assessment showing short-axis fractional area change in the absence of exogenous catecholamine stimulation: *, $p < 0.05$ vs. 4-week time point (tadalafil arm); **, $p < 0.01$ vs. HF group at 7 weeks; ***, $p < 0.001$ vs. pre-pace function (both groups). Statistics by mixed models analysis. *N* = HF, 5 at all time points; tadalafil, 20 at pre-pace, 19 at 4 weeks and 18 at 7 weeks. **E.** Representative systolic Ca^{2+} transients (left) and summary data (right); *, $p < 0.05$ vs. control; #, $p < 0.05$ vs. tadalafil. (*n/N* = 34/16 control, 7/3 HF, 24/6 Tadalafil) **F.** Summary data of echocardiographic assessments following 5 $\mu g.kg^{-1}.min^{-1}$ dobutamine infusion: **, $p < 0.01$ vs. HF by one way ANOVA. *N* = pre-pacing, 4; 4 weeks, 3; HF, 4; tadalafil, 3. **G.** Summary data showing dobutamine induced change in fractional area change derived from panel F. Data is expressed as a percentage of the maximum possible response in each group. **H.** Summary data showing RR intervals normalized to pre-dobutamine (5 μg.kg/min) RR interval: **, $p < 0.01$ vs. pre-dobutamine RR interval by t-test. *N* = pre-pacing, 5; 4 weeks, 5; HF, 6; tadalafil, 5. **I.** Paired data from 5 animals showing RR interval – dobutamine dose response relationship. *, $p < 0.05$ by mixed models analysis. Panels C – F show mean ± SEM.

Figure 2. Altered abundance of regulators of cyclic GMP in heart failure and following tadalafil treatment.

A. Summary *q*uantitative PCR assessment of myocardial brain natriuretic peptide (NPPB) mRNA abundance normalized to the housekeeper RPLPO. **B.** Summary *q*uantitative PCR assessment of myocardial phosphodiesterase 5A (PDE5A) mRNA abundance normalized to the housekeepers TBP and YWHAZ. **C.** Summary data showing

bioRxiv preprint doi: https://doi.org/10.1101/248187; this version posted January 28, 2019. The copyright holder for this preprint (which was not certified by peer review) is the author/funder. All rights reserved. No reuse allowed without permission.

no change in myocardial cGMP content. **D.** Changes in protein kinase G abundance assessed by non-denaturing PAGE showing (top) a representative blot, (middle) quantification of total and 75 kDa PKG and, (bottom) quantification of 150 kDa PKG and % total PKG as dimerized form. **E.** Altered PDE2A protein abundance showing (top) representative blot and, (bottom) summary data. **F.** Altered PDE2A protein abundance showing (top) representative blot and, (bottom) summary data. For all panels *, $p < 0.05$ vs control; #, $p < 0.05$ vs tadalafil. $N = 8$ each group.

Figure 3. Tadalafil normalizes the abundance of key regulators of β-adrenergic signalling.

A. Representative blot (upper) and summary data (lower) showing no change in β_1 adrenergic receptor abundance with tachypacing or tadalafil treatment. **B.** Representative blot (upper) and summary data (lower) showing no change in β_2 adrenergic receptor abundance with tachypacing or tadalafil treatment. **C.** Representative blot (left) and summary data (right) showing tachypacing induced increased and tadalafil mediated normalisation of GRK2 protein abundance. **D.** Representative blot (upper) and summary data (lower) showing tachypacing induced increased and tadalafil mediated normalisation of PP1 protein abundance. **E** Representative blot (upper) and summary data (lower) showing tachypacing induced increased and tadalafil mediated normalisation of PP2A protein abundance. For all panels *, $P < 0.05$ vs. control; #, $p < 0.05$ vs. tadalafil. $N = 8$ per group.

Figure 4. Recovery of transverse tubule density with altered orientation following tadalafil treatment.

A. Representative images from cell types indicated showing membrane staining (a), distance maps (b) and skeletonized images (c) from regions of interest shown in panel b. Note the reduction in TT density (a, b) and lateralization of TTs in 4-week paced, HF and tadalafil treated groups. Scale bars, 10 μm. **B.** Summary data for TT half-distance measurements. **C.** Summary data for TT fractional area measurements. For B and C: *n* cells / *N* hearts; control, 30 / 6; 4-weks, 25 / 4; HF, 29 / 6; tadalafil, 71 / 6. **D.**

bioRxiv preprint doi: https://doi.org/10.1101/248187; this version posted January 28, 2019. The copyright holder for this preprint (which was not certified by peer review) is the author/funder. All rights reserved. No reuse allowed without permission.

Representative orientation analysis for TTs in regions highlighted relative to long-axis of cells. 0° represents longitudinally orientated and 90° transversely oriented tubules. **E.** Summary data showing TT transverse to longitudinal orientation ratio. In B, C and E: *, $p < 0.05$ vs control; **, $p < 0.01$ vs. control; ***, $p < 0.001$ vs. control; #, $p < 0.05$ vs tadalafil; by linear mixed models analysis. Panels B, C & E show mean ± SEM.

Figure 5. Altered protein abundance of putative regulators of cardiac transverse tubule formation.

Representative immunoblots (upper) and summary histograms (lower) for: **A.** JPH2; **B.** TCAP and **C.** MTM1. **D.** Changes in AmpII protein abundance showing (upper) representative AmpII immunoblot and (lower) summary data (a); correlation between AmpII protein abundance and TT half distance (b) and TT fractional area (c). Solid lines through data in b. and c. are linear regressions with slopes significantly different from zero (*, $p < 0.05$). For immunoblots (A – D) N = control, 7; 4-weeks, 6; HF, 7; tadalafil, 8 and mean of 3 technical replicates. *, $p < 0.05$ vs. control; #, $p < 0.05$ vs. tadalafil; by linear mixed models analysis. For regression analysis: n cells / N hearts; control, 30/ 6; 4-weeks, 25 / 4; HF, 29 / 6; tadlafil, 71 / 6. All data presented as mean ± SEM.

bioRxiv preprint doi: https://doi.org/10.1101/248187; this version posted January 28, 2019. The copyright holder for this preprint (which was not certified by peer review) is the author/funder. All rights reserved. No reuse allowed without permission.

Figure 6. Amphiphysin II drives de novo tubule formation in neonatal rat ventricular myocytes and iPSC derived cardiac myocytes.

A. Assessment of sheep myocardial AmpII isoform expression showing (left to right) representative Qiaxcel run and summary data on sheep cardiac isoform abundance. *N* = 4 hearts. **B.** Representative immunoblot (upper) and summary data (lower) showing up-regulation of AmpII protein abundance following transient transfection of NRVMs. *N* = 2 isolations. **C.** Representative images of NRVMs transfected with mKate2 control vector (a) and AmpII expression vector (b – d). Extracellular Oregon Green 488 imaging showing a transfected and non-transfected (NT) cell (c) and overlay of the mKate2 channel (from b) and OG488N channel (from c) showing co-localisation of markers and patency of AmpII driven tubules only in the transfected cell (d). **D.** Mean data summarizing percentage of non-transfected (NT), mKate2 control vector and AmpII expression vector transfected cells with tubule structures. *N* = 6 isolations (non-transfected, 67 cells; mKate, 23 cells; AmpII, 37 cells) cells in each group. **E.** Mean data summarising fractional area of cells occupied by tubules in mKate2 control vector and AmpII expression vector transfected cells. *N* = 5 isolations (mKate2, 20 cells; AmpII, 29 cells). **F.** Representative images showing AmpII driven tubule formation in iCell iPSC derived cardiac myocytes. *N* = 2 cell batches (non-transfected, 45 cells; mKate2, 17 cells; AmpII, 40 cells). **G.** Mean data summarizing percentage of non-transfected (NT), mKate2 control vector and AmpII expression vector transfected iCell iPSC cardiac myocytes with tubule structures. **H.** Mean data summarizing fractional area occupied by tubules in iCell cardiac myocytes transfected with mKate2 or AmpII vectors. *N* = 2 cell batches (makte2, 17 cells; AmpII, 29 cells). **, $p < 0.01$ vs mKate2; ***, $p < 0.001$ vs mKate2; $^{\#}$, $p < 0.05$ vs NT; by linear mixed models analysis. Scale bars, 10 µm. Panels A, C, D, F & G show mean ± SEM.

bioRxiv preprint doi: https://doi.org/10.1101/248187; this version posted January 28, 2019. The copyright holder for this preprint (which was not certified by peer review) is the author/funder. All rights reserved. No reuse allowed without permission.

References

1 Briston, S. J. *et al.* Impaired β-adrenergic responsiveness accentuates dysfunctional excitation-contraction coupling in an ovine model of tachypacing-induced heart failure. *Journal of Physiology* **589**, 1367-1382, doi:10.1113/jphysiol.2010.203984 (2011).

2 Borlaug, B. A. *et al.* Impaired chronotropic and vasodilator reserves limit exercise capacity in patients with heart failure and a preserved ejection fraction. *Circulation* **114**, 2138-2147, doi:10.1161/CIRCULATIONAHA.106.632745 (2006).

3 Raake, P. W. J. *et al.* AAV6.βARKct cardiac gene therapy ameliorates cardiac function and normalizes the catecholaminergic axis in a clinically relevant large animal heart failure model. *Eur Heart J*, doi:10.1093/eurheartj/ehr447 (2012).

4 El-Armouche, A., Pamminger, T., Ditz, D., Zolk, O. & Eschenhagen, T. Decreased protein and phosphorylation level of the protein phosphatase inhibitor-1 in failing human hearts. *Cardiovasc Res* **61**, 87-93, doi:14732205 (2004).

5 Nikolaev, V. O. *et al.* β_2-adrenergic receptor redistribution in heart failure changes cAMP compartmentation. *Science* **327**, 1653-1657, doi:10.1126/science.1185988 (2010).

6 Laflamme, M. A. & Becker, P. L. G_s and adenylyl cyclase in transverse tubules of heart: implications for cAMP-dependent signaling. *Am J Physiol* **277**, H1841-1848 (1999).

7 Cros, C. & Brette, F. Functional subcellular distribution of β_1- and β_2-adrenergic receptors in rat ventricular cardiac myocytes. *Physiol Rep* **1**, e00038, doi:10.1002/phy2.38 (2013).

8 Caldwell, J. L. *et al.* Dependence of cardiac transverse tubules on the BAR domain protein amphiphysin II (BIN-1). *Circulation Research* **115**, 986-996, doi:10.1161/CIRCRESAHA.116.303448 (2014).

9 He, J. *et al.* Reduction in density of transverse tubules and L-type Ca^{2+} channels in canine tachycardia-induced heart failure. *Cardiovasc Res* **49**, 298-307 (2001).

10 Louch, W. E. *et al.* T-tubule disorganization and reduced synchrony of Ca^{2+} release in murine cardiomyocytes following myocardial infarction. *J Physiol* **574**, 519-533, doi:10.1113/jphysiol.2006.107227 (2006).

11 Crossman, D. J., Ruygrok, P. N., Soeller, C. & Cannell, M. B. Changes in the organization of excitation-contraction coupling structures in failing human heart. *PLoS One* **6**, e17901, doi:10.1371/journal.pone.0017901 (2011).

12 Tsai, E. J. & Kass, D. A. Cyclic GMP signaling in cardiovascular pathophysiology and therapeutics. *Pharmacol Ther* **122**, 216-238, doi:10.1016/j.pharmthera.2009.02.009 (2009).

13 Senzaki, H. *et al.* Cardiac phosphodiesterase 5 (cGMP-specific) modulates β-adrenergic signaling in vivo and is down-regulated in heart failure. *FASEB J* **15**, 1718-1726 (2001).

14 Takimoto, E. *et al.* Compartmentalization of cardiac β-adrenergic inotropy modulation by phosphodiesterase type 5. *Circulation* **115**, 2159-2167, doi:10.1161/CIRCULATIONAHA.106.643536 (2007).

15 Castro, L. R. V., Schittl, J. & Fischmeister, R. Feedback control through cGMP-dependent protein kinase contributes to differential regulation and compartmentation of cGMP in rat cardiac myocytes. *Circ Res* **107**, 1232-1240, doi:10.1161/CIRCRESAHA.110.226712 (2010).

bioRxiv preprint doi: https://doi.org/10.1101/248187; this version posted January 28, 2019. The copyright holder for this preprint (which was not certified by peer review) is the author/funder. All rights reserved. No reuse allowed without permission.

16 Takimoto, E. *et al.* cGMP catabolism by phosphodiesterase 5A regulates cardiac adrenergic stimulation by NOS3-dependent mechanism. *Circ Res* **96**, 100-109, doi:10.1161/01.RES.0000152262.22968.72 (2005).

17 Stangherlin, A. *et al.* cGMP signals modulate cAMP levels in a compartment-specific manner to regulate catecholamine-dependent signaling in cardiac myocytes. *Circ Res* **108**, 929-939, doi:10.1161/CIRCRESAHA.110.230698 (2011).

18 Mehel, H. *et al.* Phosphodiesterase-2 is up-regulated in human failing hearts and blunts β-adrenergic responses in cardiomyocytes. *J Am Coll Cardiol* **62**, 1596-1606, doi:10.1016/j.jacc.2013.05.057 (2013).

19 Anderson, S. G. *et al.* Phosphodiesterase type-5 inhibitor use in type 2 diabetes is associated with a reduction in all-cause mortality. *Heart* **102**, 1750-1756, doi:10.1136/heartjnl-2015-309223 (2016).

20 Giannetta, E. *et al.* Is chronic inhibition of phosphodiesterase type 5 cardioprotective and safe? A meta-analysis of randomized controlled trials. *BMC Med* **12**, 185, doi:10.1186/s12916-014-0185-3 (2014).

21 Guazzi, M., Vicenzi, M., Arena, R. & Guazzi, M. D. PDE5 inhibition with sildenafil improves left ventricular diastolic function, cardiac geometry, and clinical status in patients with stable systolic heart failure: results of a 1-year, prospective, randomized, placebo-controlled study. *Circ Heart Fail* **4**, 8-17, doi:10.1161/CIRCHEARTFAILURE.110.944694 (2011).

22 Xie, Y.-P. *et al.* Sildenafil prevents and reverses transverse-tubule remodeling and Ca^{2+} handling dysfunction in right ventricle failure induced by pulmonary artery hypertension. *Hypertension* **59**, 355-362, doi:10.1161/HYPERTENSIONAHA.111.180968 (2012).

23 Salloum, F. N. *et al.* Sildenafil (Viagra) attenuates ischemic cardiomyopathy and improves left ventricular function in mice. *Am J Physiol Heart Circ Physiol* **294**, H1398-1406, doi:10.1152/ajpheart.91438.2007 (2008).

24 Nagy, O., Hajnal, A., Parratt, J. R. & Végh, A. Sildenafil (Viagra) reduces arrhythmia severity during ischaemia 24 h after oral administration in dogs. *Br J Pharmacol* **141**, 549-551, doi:10.1038/sj.bjp.0705658 (2004).

25 Ockaili, R., Salloum, F., Hawkins, J. & Kukreja, R. C. Sildenafil (Viagra) induces powerful cardioprotective effect via opening of mitochondrial K_{ATP} channels in rabbits. *Am J Physiol Heart Circ Physiol* **283**, H1263-1269, doi:10.1152/ajpheart.00324.2002 (2002).

26 Reffelmann, T. & Kloner, R. A. Effects of sildenafil on myocardial infarct size, microvascular function, and acute ischemic left ventricular dilation. *Cardiovasc Res* **59**, 441-449 (2003).

27 Huang, C. K. *et al.* Sildenafil ameliorates left ventricular T-tubule remodeling in a pressure overload-induced murine heart failure model. *Acta Pharmacol Sin* **37**, 473-482, doi:10.1038/aps.2016.13 (2016).

28 Takimoto, E. *et al.* Chronic inhibition of cyclic GMP phosphodiesterase 5A prevents and reverses cardiac hypertrophy. *Nat Med* **11**, 214-222, doi:10.1038/nm1175 (2005).

29 Nagayama, T. *et al.* Sildenafil stops progressive chamber, cellular, and molecular remodeling and improves calcium handling and function in hearts with pre-existing advanced hypertrophy caused by pressure overload. *J Am Coll Cardiol* **53**, 207-215, doi:10.1016/j.jacc.2008.08.069 (2009).

bioRxiv preprint doi: https://doi.org/10.1101/248187; this version posted January 28, 2019. The copyright holder for this preprint (which was not certified by peer review) is the author/funder. All rights reserved. No reuse allowed without permission.

30 Eskesen, K. *et al.* Sildenafil treatment attenuates ventricular remodeling in an experimental model of aortic regurgitation. *Springerplus* **4**, 592, doi:10.1186/s40064-015-1317-8 (2015).
31 Hobai, I. A. & O'Rourke, B. Decreased sarcoplasmic reticulum calcium content is responsible for defective excitation-contraction coupling in canine heart failure. *Circulation* **103**, 1577-1584, doi:11257088 (2001).
32 Forgue, S. T. *et al.* Tadalafil pharmacokinetics in healthy subjects. *Br J Clin Pharmacol* **61**, 280-288, doi:10.1111/j.1365-2125.2005.02553.x (2006).
33 Horn, M. A. *et al.* Temporal Development of Autonomic Dysfunction in Heart Failure: Effects of Age in an Ovine Rapid-pacing Model. *J Gerontol A Biol Sci Med Sci*, doi:10.1093/gerona/glv217 (2015).
34 Dibb, K. M. *et al.* Characterization of an extensive transverse tubular network in sheep atrial myocytes and its depletion in heart failure. *Circ Heart Fail* **2**, 482-489, doi:10.1161/CIRCHEARTFAILURE.109.852228 (2009).
35 Clarke, J. D. *et al.* Perturbed atrial calcium handling in an ovine model of heart failure: Potential roles for reductions in the L-type calcium current. *J Mol Cell Cardiol* **79**, 169-179, doi:10.1016/j.yjmcc.2014.11.017 (2015).
36 Horn, M. A. *et al.* Age-related divergent remodeling of the cardiac extracellular matrix in heart failure: Collagen accumulation in the young and loss in the aged. *Journal of Molecular and Cellular Cardiology* **53**, 82-90, doi:10.1016/j.yjmcc.2012.03.011 (2012).
37 Coletta, C. *et al.* Prognostic value of left ventricular volume response during dobutamine stress echocardiography. *Eur Heart J* **18**, 1599-1605 (1997).
38 Hiemstra, J. A. *et al.* Saxagliptin and Tadalafil Differentially Alter Cyclic Guanosine Monophosphate (cGMP) Signaling and Left Ventricular Function in Aortic-Banded Mini-Swine. *J Am Heart Assoc* **5**, e003277, doi:10.1161/JAHA.116.003277 (2016).
39 Zhou, Z. *et al.* Protein kinase G phosphorylates soluble guanylyl cyclase on serine 64 and inhibits its activity. *Arterioscler Thromb Vasc Biol* **28**, 1803-1810, doi:10.1161/ATVBAHA.108.165043 (2008).
40 Wei, S. *et al.* T-Tubule Remodeling During Transition From Hypertrophy to Heart Failure. *Circ Res* **107**, 521-531, doi:10.1161/CIRCRESAHA.109.212324 (2010).
41 Hong, T.-T. *et al.* BIN1 is reduced and Cav1.2 trafficking is impaired in human failing cardiomyocytes. *Heart Rhythm* **9**, 812-820, doi:10.1016/j.hrthm.2011.11.055 (2012).
42 Hong, T. *et al.* Cardiac BIN1 folds T-tubule membrane, controlling ion flux and limiting arrhythmia. *Nature Medicine* **20**, 624-632, doi:10.1038/nm.3543 (2014).
43 Bischoff, E. Potency, selectivity, and consequences of nonselectivity of PDE inhibition. *Int J Impot Res* **16 Suppl 1**, S11-14, doi:10.1038/sj.ijir.3901208 (2004).
44 Zhang, X., Feng, Q. & Cote, R. H. Efficacy and selectivity of phosphodiesterase-targeted drugs in inhibiting photoreceptor phosphodiesterase (PDE6) in retinal photoreceptors. *Invest Ophthalmol Vis Sci* **46**, 3060-3066, doi:10.1167/iovs.05-0257 (2005).
45 Wright, P. J. Comparison of phosphodiesterase type 5 (PDE5) inhibitors. *Int J Clin Pract* **60**, 967-975, doi:10.1111/j.1742-1241.2006.01049.x (2006).
46 Weeks, J. L. *et al.* High biochemical selectivity of tadalafil, sildenafil and vardenafil for human phosphodiesterase 5A1 (PDE5) over PDE11A4 suggests the absence of PDE11A4 cross-reaction in patients. *Int J Impot Res* **17**, 5-9, doi:10.1038/sj.ijir.3901283 (2005).

bioRxiv preprint doi: https://doi.org/10.1101/248187; this version posted January 28, 2019. The copyright holder for this preprint (which was not certified by peer review) is the author/funder. All rights reserved. No reuse allowed without permission.

47 Loughney, K., Taylor, J. & Florio, V. A. 3',5'-cyclic nucleotide phosphodiesterase 11A: localization in human tissues. *Int J Impot Res* **17**, 320-325, doi:10.1038/sj.ijir.3901317 (2005).

48 Mehrotra, N., Gupta, M., Kovar, A. & Meibohm, B. The role of pharmacokinetics and pharmacodynamics in phosphodiesterase-5 inhibitor therapy. *Int J Impot Res* **19**, 253-264, doi:10.1038/sj.ijir.3901522 (2007).

49 Chau, V. Q., Salloum, F. N., Hoke, N. N., Abbate, A. & Kukreja, R. C. Mitigation of the progression of heart failure with sildenafil involves inhibition of RhoA/Rho-kinase pathway. *Am J Physiol Heart Circ Physiol* **300**, H2272-2279, doi:10.1152/ajpheart.00654.2010 (2011).

50 Westermann, D. *et al.* Selective PDE5A inhibition with sildenafil rescues left ventricular dysfunction, inflammatory immune response and cardiac remodeling in angiotensin II-induced heart failure in vivo. *Basic Res Cardiol* **107**, 308, doi:10.1007/s00395-012-0308-y (2012).

51 Chakir, K. *et al.* Mechanisms of enhanced β-adrenergic reserve from cardiac resynchronization therapy. *Circulation* **119**, 1231-1240, doi:10.1161/CIRCULATIONAHA.108.774752 (2009).

52 Nikolaev, V. O., Bünemann, M., Schmitteckert, E., Lohse, M. J. & Engelhardt, S. Cyclic AMP imaging in adult cardiac myocytes reveals far-reaching β1-adrenergic but locally confined β2-adrenergic receptor-mediated signaling. *Circ Res* **99**, 1084-1091, doi:10.1161/01.RES.0000250046.69918.d5 (2006).

53 Katz, M. G. *et al.* AAV6-βARKct gene delivery mediated by molecular cardiac surgery with recirculating delivery (MCARD) in sheep results in robust gene expression and increased adrenergic reserve. *J Thorac Cardiovasc Surg* **143**, 720-726.e723, doi:10.1016/j.jtcvs.2011.08.048 (2012).

54 Carr, A. N. *et al.* Type 1 phosphatase, a negative regulator of cardiac function. *Mol Cell Biol* **22**, 4124-4135 (2002).

55 Wijnker, P. J. *et al.* Protein phosphatase 2A affects myofilament contractility in non-failing but not in failing human myocardium. *J Muscle Res Cell Motil* **32**, 221-233, doi:10.1007/s10974-011-9261-x (2011).

56 Lei, M., Wang, X., Ke, Y. & Solaro, R. J. Regulation of Ca^{2+} transient by PP2A in normal and failing heart. *Front Physiol* **6**, 13, doi:10.3389/fphys.2015.00013 (2015).

57 Seidel, T. *et al.* Sheet-Like Remodeling of the Transverse Tubular System in Human Heart Failure Impairs Excitation-Contraction Coupling and Functional Recovery by Mechanical Unloading. *Circulation*, doi:10.1161/CIRCULATIONAHA.116.024470 (2017).

58 Lenaerts, I. *et al.* Ultrastructural and functional remodeling of the coupling between Ca^{2+} influx and sarcoplasmic reticulum Ca^{2+} release in right atrial myocytes from experimental persistent atrial fibrillation. *Circ Res* **105**, 876-885, doi:10.1161/CIRCRESAHA.109.206276 (2009).

59 Wagner, E. *et al.* Stimulated emission depletion live-cell super-resolution imaging shows proliferative remodeling of T-tubule membrane structures after myocardial infarction. *Circ Res* **111**, 402-414, doi:10.1161/CIRCRESAHA.112.274530 (2012).

60 Frisk, M. *et al.* Elevated ventricular wall stress disrupts cardiomyocyte t-tubule structure and calcium homeostasis. *Cardiovasc Res* **112**, 443-451, doi:10.1093/cvr/cvw111 (2016).

bioRxiv preprint doi: https://doi.org/10.1101/248187; this version posted January 28, 2019. The copyright holder for this preprint (which was not certified by peer review) is the author/funder. All rights reserved. No reuse allowed without permission.

61 McNary, T. G., Bridge, J. H. & Sachse, F. B. Strain transfer in ventricular cardiomyocytes to their transverse tubular system revealed by scanning confocal microscopy. *Biophys J* **100**, L53-55, doi:10.1016/j.bpj.2011.03.046 (2011).

62 Li, H. *et al.* Cardiac Resynchronization Therapy Reduces Subcellular Heterogeneity of Ryanodine Receptors, T-Tubules, and Ca^{2+} Sparks Produced by Dyssynchronous Heart Failure. *Circ Heart Fail* **8**, 1105-1114, doi:10.1161/CIRCHEARTFAILURE.115.002352 (2015).

63 Lyon, A. R. *et al.* Plasticity of Surface Structures and β_2-Adrenergic Receptor Localization in Failing Ventricular Cardiomyocytes During Recovery from Heart Failure. *Circ Heart Fail* **5**, 357-365, doi:10.1161/CIRCHEARTFAILURE.111.964692 (2012).

64 Ibrahim, M. *et al.* Mechanical unloading reverses transverse tubule remodelling and normalizes local Ca^{2+}-induced Ca^{2+}release in a rodent model of heart failure. *Eur J Heart Fail* **14**, 571-580, doi:10.1093/eurjhf/hfs038 (2012).

65 Ibrahim, M., Gorelik, J., Yacoub, M. H. & Terracciano, C. M. The structure and function of cardiac t-tubules in health and disease. *Proc Biol Sci* **278**, 2714-2723, doi:10.1098/rspb.2011.0624 (2011).

66 Dowling, J. J. *et al.* Loss of myotubularin function results in T-tubule disorganization in zebrafish and human myotubular myopathy. *PLoS Genet* **5**, e1000372, doi:10.1371/journal.pgen.1000372 (2009).

67 Al-Qusairi, L. & Laporte, J. T-tubule biogenesis and triad formation in skeletal muscle and implication in human diseases. *Skelet Muscle* **1**, 26, doi:10.1186/2044-5040-1-26 (2011).

68 Razzaq, A. *et al.* Amphiphysin is necessary for organization of the excitation-contraction coupling machinery of muscles, but not for synaptic vesicle endocytosis in Drosophila. *Genes Dev* **15**, 2967-2979, doi:10.1101/gad.207801 (2001).

69 Hong, T.-T. *et al.* BIN1 localizes the L-type calcium channel to cardiac T-tubules. *PLoS Biol* **8**, e1000312, doi:10.1371/journal.pbio.1000312 (2010).

70 De La Mata, A. *et al.* BIN1 induces the formation of T-tubules and adult-like Ca(2+) release units in developing cardiomyocytes. *Stem Cells*, doi:10.1002/stem.2927 (2018).

71 Wechsler-Reya, R., Sakamuro, D., Zhang, J., Duhadaway, J. & Prendergast, G. C. Structural analysis of the human BIN1 gene. Evidence for tissue-specific transcriptional regulation and alternate RNA splicing. *J Biol Chem* **272**, 31453-31458 (1997).

72 Richards, M. A. *et al.* Transverse (t-) tubules are a common feature in large mammalian atrial myocytes including human. *Am J Physiol Heart Circ Physiol* **301**, H1996-2005, doi:10.1152/ajpheart.00284.2011 (2011).

73 Agrawal, P. B. *et al.* SPEG interacts with myotubularin, and its deficiency causes centronuclear myopathy with dilated cardiomyopathy. *Am J Hum Genet* **95**, 218-226, doi:10.1016/j.ajhg.2014.07.004 (2014).

74 Royer, B. *et al.* The myotubularin-amphiphysin 2 complex in membrane tubulation and centronuclear myopathies. *EMBO Rep* **14**, 907-915, doi:10.1038/embor.2013.119 (2013).

75 Kutchukian, C. *et al.* Phosphatidylinositol 3-kinase inhibition restores Ca^{2+} release defects and prolongs survival in myotubularin-deficient mice. *Proc Natl Acad Sci U S A* **113**, 14432-14437, doi:10.1073/pnas.1604099113 (2016).

bioRxiv preprint doi: https://doi.org/10.1101/248187; this version posted January 28, 2019. The copyright holder for this preprint (which was not certified by peer review) is the author/funder. All rights reserved. No reuse allowed without permission.

76 Al-Qusairi, L. *et al.* T-tubule disorganization and defective excitation-contraction coupling in muscle fibers lacking myotubularin lipid phosphatase. *Proc Natl Acad Sci U S A* **106**, 18763-18768, doi:10.1073/pnas.0900705106 (2009).

77 Kilkenny, C., Browne, W. J., Cuthill, I. C., Emerson, M. & Altman, D. G. Improving bioscience research reporting: the ARRIVE guidelines for reporting animal research. *PLoS Biol* **8**, e1000412, doi:10.1371/journal.pbio.1000412 (2010).

78 Pinali, C., Bennett, H., Davenport, J. B., Trafford, A. W. & Kitmitto, A. 3-D Reconstruction of the Cardiac Sarcoplasmic Reticulum Reveals a Continuous Network Linking T-Tubules: This Organization is Perturbed in Heart Failure. *Circ Res* **113**, 1219-1230, doi:10.1161/CIRCRESAHA.113.301348 (2013).

79 Greensmith, D. J., Galli, G. L. J., Trafford, A. W. & Eisner, D. A. Direct measurements of SR free Ca reveal the mechanism underlying the transient effects of RyR potentiation under physiological conditions. *Cardiovasc Res* **103**, 554-563, doi:10.1093/cvr/cvu158 (2014).

80 Trafford, A. W., O'Neill, S. C. & Eisner, D. A. Factors affecting the propagation of locally activated systolic Ca transients in rat ventricular myocytes. *Pflugers Arch* **425**, 181-183 (1993).

81 Walden, A. P., Dibb, K. M. & Trafford, A. W. Differences in intracellular calcium homeostasis between atrial and ventricular myocytes. *J Mol Cell Cardiol* **46**, 463-473, doi:10.1016/j.yjmcc.2008.11.003 (2009).

82 Kim, K.-Y. *et al.* Validated UPLC-MS/MS method for the determination of tadalafil in human plasma and its application to a pharmacokinetic study. *Trans Clin Pharmacol* **25**, 21-27, doi:https://doi.org/10.12793/tcp.2017.25.1.21 (2017).

83 Keene, O. N. The log transformation is special. *Stat Med* **14**, 811-819 (1995).